Self-Organized Formation of Retinotopic Projections Between Manifolds of Different Geometries – Part 2: Euclidean Manifolds

M. Güßmann* and G. Wunner†
1. Institut für Theoretische Physik, Universität Stuttgart, Pfaffenwaldring 57, 70569 Stuttgart, Germany

A. Pelster‡
Fachbereich Physik, Campus Essen, Universität Duisburg-Essen, Universitätsstrasse 5, 45117 Essen, Germany
(Dated: July 31, 2006)

We apply generic order parameter equations for the emergence of retinotopy between manifolds of different geometry derived in part 1 of this series of papers to one- and two-dimensional Euclidean manifolds. Our results for strings are analogous to those for discrete linear chains obtained previously by Häussler and von der Malsburg. The case of planes turns out to be more involved as the two dimensions do not decouple in a trivial way. However, superimposing two modes under suitable conditions provides a state with a pronounced retinotopic character.

PACS numbers: 05.45.-a, 87.18.Hf, 89.75.Fb

arXiv:physics/0607259 v1 28 Jul 2006

I. INTRODUCTION

In a preceding paper [1] we have developed, using the methods of synergetics, a general model for the formation of retinotopic projections independent of geometry and dimension. In this paper we discuss, as a first application of the general model, Euclidean geometries in one and two dimensions. To put these investigations into perspective we briefly recall their physiological motivations. In the course of ontogenesis of vertebrate animals well-ordered neural connections are established between retina and tectum, a part of the brain which plays an important role in processing optical information. At an initial stage of ontogenesis, the ganglion cells of the retina have random synaptic contacts with the tectum. In the adult animal, however, neighbouring retinal cells project onto neighbouring cells of the tectum [2]. A detailed analytical treatment by Häussler and von der Malsburg was able to describe the generation of such retinotopic states from an undifferentiated initial state as a self-organization process [3]. In that work retina and tectum were treated as one-dimensional discrete cell arrays. The dynamics of the connection weights between retina and tectum was assumed to be governed by the so-called Häussler equations which are based on modelling the interplay between cooperative and competitive interactions of the individual synaptic contacts. The analysis was performed by using the methods of synergetics, which provides effective analytical methods to study self-organization processes in complex systems [4, 5].

Obviously, the description of cell sheets as linear chains with the same number of cells is an inadequate approach to the real biological situation. In the preceding paper of this series we generalized the underlying Häussler equations to *continuous* manifolds of *arbitrary* geometry and dimension in Ref. [1]. We performed an extensive synergetic analysis of these generalized Häussler equations. The resulting generic order parameter equations represented a central new result and can now serve as a starting point to analyze in detail the self-organized emergence of one-to-one mappings in cell arrays of different geometries. A brief survey of our generalization of the Häussler equations and the results of the corresponding synergetic analysis is provided in Section II.

In this paper we focus on the modelling of retina and tectum as one- and two-dimensional Euclidean manifolds. We show in Section III that the treatment of strings yields results which are analogous to those obtained for discrete linear chains in Ref. [3], i.e. our model includes the special case discussed by Häussler and von der Malsburg. However, our synergetic analysis is more general. Instead of discrete cell arrays with the same number of cells, we consider continuously distributed cells on strings of different lengths [6]. Furthermore, we do not restrict our investigations to monotonically decreasing cooperativity functions of strings. We investigate under what circumstances non-retinotopic

*Electronic address: martin.guessmann@itp1.uni-stuttgart.de
†Electronic address: guenter.wunner@itp1.uni-stuttgart.de
‡Electronic address: axel.pelster@uni-due.de

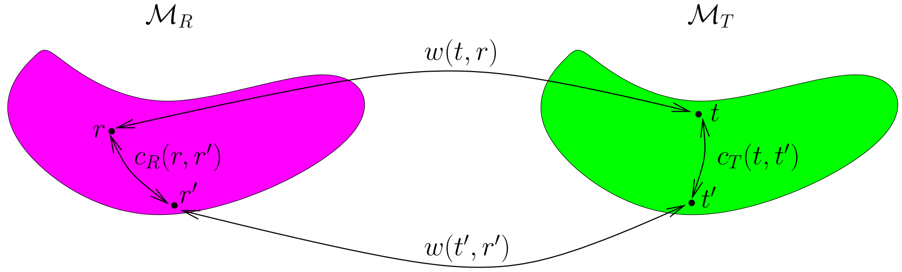

FIG. 1: Retina and tectum are represented as manifolds $\mathcal{M}_R$ and $\mathcal{M}_T$, respectively, which are connected by positive connection weights $w(t,r)$. The connectivity within each manifold is represented by cooperativity functions $c_R(r,r')$ and $c_T(t,t')$.

modes become unstable and destroy retinotopic order. Finally, we show in Section IV that our generic order parameter equations also provide a suitable framework to describe the emergence of retinotopy between planes.

II. THE GENERAL MODEL

To make the present paper self-contained, we briefly review the essential results of our general model for the self-organized emergence of retinotopic projections between manifolds of different geometry in Ref. [1]. The two cell sheets, retina and tectum, are represented by general manifolds $\mathcal{M}_R$ and $\mathcal{M}_T$, respectively. Every ordered pair (t,r) with $t \in \mathcal{M}_T$, $r \in \mathcal{M}_R$ is connected by a connection weight $w(t,r)$ as is illustrated in Figure 1. The equations of evolution of these connection weights are assumed to be given by a generalization of the *Häussler equations*

$$\dot{w}(t,r) = f(t,r,w) - \frac{w(t,r)}{2M_T} \int dt'\, f(t',r,w) - \frac{w(t,r)}{2M_R} \int dr'\, f(t,r',w)\,, \tag{1}$$

where the first term on the right-hand side describes cooperative synaptic growth processes and the other terms stand for corresponding competitive growth processes. Here the total growth rates are defined by

$$f(t,r,w) = \alpha + w(t,r) \int dt' \int dr' c_T(t,t')\, c_R(r,r')\, w(t',r') \tag{2}$$

and α denotes the global growth rate of new synapses onto the tectum which represents the control parameter of our system. The cooperativity functions $c_T(t,t')$, $c_R(r,r')$ represent the neural connectivity within each manifold. We assume that they are positive, symmetric with respect to their arguments and normalized. The cooperation strength depends on the distance between two points of the manifold. This requires a measure of distance, i.e. metrices, which in turn define Laplace-Beltrami operators on the manifolds. Their eigenvalue problems yield a complete orthonormal system $\psi_{\lambda_T}(t)\,,\psi_{\lambda_R}(r)$, and the generalized Häussler equations are most conveniently transformed to this new basis. For example, the cooperativity functions are expanded in terms of these functions as follows:

$$c_T(t,t') = \sum_{\lambda_T} f_{\lambda_T} \psi_{\lambda_T}(t) \psi^*_{\lambda_T}(t')\,, \qquad c_R(r,r') = \sum_{\lambda_R} f_{\lambda_R} \psi_{\lambda_R}(r) \psi^*_{\lambda_R}(r')\,. \tag{3}$$

The initial state of ontogenesis with randomly distributed synaptic contacts is described by the stationary uniform solution of the generalized Häussler equations $w_0(t,r) = 1$. Its stability is analyzed by linearizing the Häussler equations (1) with respect to the deviation $v(t,r) = w(t,r) - w_0(t,r)$. The resulting linearized equations read

$$\dot{v}(t,r) = \hat{L}(t,r,v) \tag{4}$$

with the linear operator

$$\begin{aligned}\hat{L}(t,r,v) = -\alpha v(r,v) - \frac{1}{2M_T} \int dt' \left[v(t',r) + \int dt'' \int dr''\, c_T(t',t'')\, c_R(r,r'')\, v(t'',r'') \right] \\ -\frac{1}{2M_R} \int dr' \left[v(t,r') + \int dt'' \int dr''\, c_T(t,t'')\, c_R(r',r'')\, v(t'',r'') \right] + \int dt' \int dr'\, c_T(t,t')\, c_R(r,r')\, v(t',r')\,.\end{aligned} \tag{5}$$

To solve Eq. (4), we have to consider the eigenvalue problem of the linear operator (5). It has the eigenfunctions

$$v_{\lambda_T \lambda_R}(t,r) = \psi_{\lambda_T}(t) \psi_{\lambda_R}(r) \tag{6}$$

and the following spectrum of eigenvalues:

$$\Lambda_{\lambda_T\lambda_R} = \begin{cases} -\alpha - 1 & \lambda_T = \lambda_R = 0 \\ -\alpha + \frac{1}{2}(f^T_{\lambda_T} f^R_{\lambda_R} - 1) & \lambda_T = 0, \lambda_R \neq 0; \lambda_R = 0, \lambda_T \neq 0 \\ -\alpha + f^T_{\lambda_T} f^R_{\lambda_R} & \text{otherwise.} \end{cases} \tag{7}$$

The maximum eigenvalue is given by $\Lambda_{\max} = -\alpha + f^T_{\lambda^u_T} f^R_{\lambda^u_R}$, where λ^u_T, λ^u_R denote those eigenvalues which could become unstable. Thus, the instability takes place when the global growth rate reaches its critical value $\alpha_c = f^T_{\lambda^u_T} f^R_{\lambda^u_R}$.

The linear stability analysis motivates to treat the nonlinear Häussler equations (1) near the instability by decomposing the deviation $v(t, r) = w(t, r) - w_0(t, r)$ in unstable and stable contributions according to

$$v(t, r) = U(t, r) + S(t, r)\,. \tag{8}$$

With Einstein's sum convention we have for the unstable modes

$$U(t, r) = U_{\lambda^u_T\lambda^u_R}\psi_{\lambda^u_T}(t)\psi_{\lambda^u_R}(r)\,, \tag{9}$$

and, correspondingly,

$$S(t, r) = S_{\lambda_T\lambda_R}\,\psi_{\lambda_T}(t)\psi_{\lambda_R}(r) \tag{10}$$

represents the contribution of the stable modes. Note that the summation in (10) is performed over all parameters $(\lambda_T; \lambda_R)$ except for $(\lambda^u_T; \lambda^u_R)$, i.e. from now on the parameters $(\lambda_T; \lambda_R)$ stand for the stable modes alone. With the help of the slaving principle of synergetics the original high-dimensional system can be reduced to a low-dimensional one which only contains the unstable amplitudes. The general form of the resulting order parameter equations is independent of the geometry of the problem and reads

$$\dot{U}_{\lambda^u_T\lambda^u_R} \;=\; \Lambda_{\lambda^u_T\lambda^u_R}\,U_{\lambda^u_T\lambda^u_R} + A^{\lambda^u_T,\lambda^u_T{}'\lambda^u_T{}''}_{\lambda^u_R,\lambda^u_R{}'\lambda^u_R{}''}\,U_{\lambda^u_T{}'\lambda^u_R{}'}\,U_{\lambda^u_T{}''\lambda^u_R{}''} + B^{\lambda^u_T,\lambda^u_T{}'\lambda^u_T{}''\lambda^u_T{}'''}_{\lambda^u_R,\lambda^u_R{}'\lambda^u_R{}''\lambda^u_R{}'''}U_{\lambda^u_T{}'\lambda^u_R{}'}\,U_{\lambda^u_T{}''\lambda^u_R{}''}\,U_{\lambda^u_T{}'''\lambda^u_R{}'''}\,. \tag{11}$$

It contains, as is typical, a linear, a quadratic, and a cubic term of the order parameters. The corresponding coefficients can be expressed in terms of the expansion coefficients f_{λ_T}, f_{λ_R} of the cooperativity functions (3) and integrals over products of the eigenfunctions $\psi_{\lambda_T}(t)$, $\psi_{\lambda_R}(r)$:

$$I^{\lambda}_{\lambda^{(1)}\lambda^{(2)}\ldots\lambda^{(n)}} \;=\; \int dx\,\psi^*_\lambda(x)\,\psi_{\lambda^{(1)}}(x)\,\psi_{\lambda^{(2)}}(x)\,\cdots\,\psi_{\lambda^{(n)}}(x)\,, \tag{12}$$

$$J_{\lambda^{(1)}\lambda^{(2)}\ldots\lambda^{(n)}} \;=\; \int dx\,\psi_{\lambda^{(1)}}(x)\,\psi_{\lambda^{(2)}}(x)\,\cdots\,\psi_{\lambda^{(n)}}(x)\,. \tag{13}$$

The quadratic coefficients read

$$A^{\lambda^u_T,\lambda^u_T{}'\lambda^u_T{}''}_{\lambda^u_R,\lambda^u_R{}'\lambda^u_R{}''} = f_{\lambda^u_T{}''}\,f_{\lambda^u_R{}''}\,I^{\lambda^u_T}_{\lambda^u_T{}'\lambda^u_T{}''}\,I^{\lambda^u_R}_{\lambda^u_R{}'\lambda^u_R{}''}\,, \tag{14}$$

whereas the cubic coefficients are

$$\begin{aligned} B^{\lambda^u_T,\lambda^u_T{}'\lambda^u_T{}''\lambda^u_T{}'''}_{\lambda^u_R,\lambda^u_R{}'\lambda^u_R{}''\lambda^u_R{}'''} \;=\; & -\frac{1}{2}\,f_{\lambda^u_T{}'''}\,f_{\lambda^u_R{}'''}\left(\frac{1}{M_R}\,I^{\lambda^u_T}_{\lambda^u_T{}'\lambda^u_T{}''\lambda^u_T{}'''}\,\delta_{\lambda^u_R\lambda^u_R{}'}\,J_{\lambda^u_R{}''\lambda^u_R{}'''} + \frac{1}{M_T}\,I^{\lambda^u_R}_{\lambda^u_R{}'\lambda^u_R{}''\lambda^u_R{}'''}\delta_{\lambda^u_T\lambda^u_T{}'}\,J_{\lambda^u_T{}''\lambda^u_T{}'''}\right) \\ & + \Bigg\{\left[f_{\lambda_T}\,f_{\lambda_R} + f_{\lambda^u_T{}'}\,f_{\lambda^u_R{}'}\right]I^{\lambda^u_T}_{\lambda^u_T{}'\lambda_T}\,I^{\lambda^u_R}_{\lambda^u_R{}'\lambda_R} - \frac{1}{2}\,\Bigg[\,\frac{1}{\sqrt{M_T}}\,\delta_{\lambda_T 0}\,\delta_{\lambda^u_T\lambda^u_T{}'}\,\left(1 + f_{\lambda_R}\right)I^{\lambda^u_R}_{\lambda^u_R{}'\lambda_R} \\ & + \frac{1}{\sqrt{M_R}}\,\delta_{\lambda_R 0}\,\delta_{\lambda^u_R\lambda^u_R{}'}\,\left(1 + f_{\lambda_T}\right)\,I^{\lambda^u_T}_{\lambda^u_T{}'\lambda_T}\Bigg]\Bigg\}\,H^{\lambda_T\lambda_R}_{\lambda^u_T{}''\lambda^u_R{}'',\lambda^u_T{}'''\lambda^u_R{}'''}\,. \end{aligned} \tag{15}$$

As is common in synergetics, the cubic coefficients (15) consist in general of two parts, one stemming from the order parameters themselves and the other representing the influence of the center manifold H on the order parameter dynamics according to

$$S_{\lambda_T\lambda_R} = H^{\lambda_T\lambda_R}_{\lambda^u_T\lambda^u_R,\lambda^u_T{}'\lambda^u_R{}'}\,U_{\lambda^u_T\lambda^u_R}U_{\lambda^u_T{}'\lambda^u_R{}'}\,. \tag{16}$$

Here the center manifold coefficients $H^{\lambda_T \lambda_R}_{\lambda^u_T \lambda^u_R, \lambda^u_T{}' \lambda^u_R{}'}$ are defined by

$$H^{\lambda_T \lambda_R}_{\lambda^u_T \lambda^u_R, \lambda^u_T{}' \lambda^u_R{}'} = \frac{f_{\lambda^u_T{}'} f_{\lambda^u_R{}'}}{\Lambda_{\lambda^u_T \lambda^u_R} + \Lambda_{\lambda^u_T{}' \lambda^u_R{}'} - \Lambda_{\lambda_T \lambda_R}} \Bigg[I^{\lambda_T}_{\lambda^u_T \lambda^u_T{}'} I^{\lambda_R}_{\lambda^u_R \lambda^u_R{}'} - \frac{1}{2} \left(\frac{1}{\sqrt{M_T}} J_{\lambda^u_T \lambda^u_T{}'} I^{\lambda_R}_{\lambda^u_R \lambda^u_R{}'} \delta_{\lambda_T 0} + \frac{1}{\sqrt{M_R}} J_{\lambda^u_R \lambda^u_R{}'} I^{\lambda_T}_{\lambda^u_T \lambda^u_T{}'} \delta_{\lambda_R 0} \right) \Bigg] . \tag{17}$$

The order parameter equations (11) for the generalized Häussler equations (1) can now serve as a starting point for analysing the self-organized formation of retinotopic projections between manifolds of different geometry.

III. STRINGS

In this section we specialize the generic order parameter equations (11) to one-dimensional Euclidean manifolds of strings with different lengths L_T and L_R. We observe that the quadratic term vanishes and derive selection rules for the appearance of cubic terms. In this way we essentially simplify the calculation of order parameter equations as compared with Ref. [3]. Furthermore, we show that the order parameter equations represent a potential dynamics, and determine the underlying potential. A subsequent transformation from complex to real order parameters leads to constant phase-shift angles. This allows us to reduce the order parameter dynamics to two variables which correspond to the amplitudes of two diagonal modes. These two modes compete with each other, until one of them vanishes. Within the potential picture this means that the originally stable uniform state becomes unstable and the system settles in one of the two potential minima. After one of the diagonal modes has won, only such modes are excited which contribute to the sharpening of the diagonal. Approximately solving the Häussler equations leads to the following scenario: Above a critical global growth rate α_c the uniform state $w_0(t,r) = 1$ is stable. By decreasing the control parameter α, the projection gets sharper and sharper. Finally, if there is no global growth rate of new synapses any more, i.e. $\alpha = 0$, the connection weights are given by Dirac's delta function. Thus, a perfect one-to-one retinotopic state is realized.

A. Eigenfunctions

The magnitudes of the manifolds $\mathcal{M}_T$ and $\mathcal{M}_R$ are given by $M_T = L_T$ and $M_R = L_R$, respectively. To avoid problems at the boundaries, we assume periodic boundary conditions, i.e. we consider retina and tectum to be rings with circumferences L_T and L_R, respectively. The eigenvalue problem of the Laplace-Beltrami operator for both manifolds reads

$$\frac{\partial^2}{\partial x^2} \psi_\lambda(x) = \chi_\lambda \psi_\lambda(x) , \tag{18}$$

with $x = t, r$, respectively. Using the boundary condition $\psi_\lambda(x) = \psi_\lambda(x + L)$, this is solved by the eigenfunctions

$$\psi_\lambda(x) = \frac{1}{\sqrt{L}} \exp\left(i \frac{2\pi}{L} \lambda x \right) , \tag{19}$$

where the eigenvalues are given by

$$\chi_\lambda = -\frac{4\pi^2}{L^2} \lambda^2 \tag{20}$$

with $x \in [0, L)$ and $\lambda = 0, \pm 1, \pm 2, \ldots$. Every eigenvalue χ_λ, apart from the special case $\chi_0 = 0$, is two-fold degenerate. The eigenfunctions form a complete orthonormal system:

$$\int_0^L dx \, \psi_\lambda(x) \psi^*_{\lambda'}(x) = \delta_{\lambda\lambda'} , \tag{21}$$

$$\sum_{\lambda=-\infty}^{\infty} \psi_\lambda(x) \psi^*_\lambda(x') = \delta(x - x') . \tag{22}$$

Note that the orthonormality relation (21) follows directly by inserting (19) into (21), whereas the completeness relation (22) is proven by taking into account the Poisson formula [7]. The cooperativity functions only depend on the distance, which is given by the Euclidean distance $|x - x'|$, i.e. $c(x, x') = c(x - x')$. Their expansion in terms of the eigenfunctions (19) corresponds to the Fourier series

$$c(x - x') = \frac{1}{L} \sum_{\lambda=-\infty}^{\infty} f_\lambda \exp\left[i \frac{2\pi}{L} \lambda \, (x - x') \right] . \tag{23}$$

The expansion coefficients f_λ are independent of the sign of the parameters λ, i.e. $f_\lambda = f_{-\lambda}$, as the cooperativity functions are symmetric with respect to their arguments: $c(x - x') = c(x' - x)$.

B. Synergetic Analysis

To specialize the order parameter equations (11) to the case of strings, we have to determine the integrals (12) and (13) of products of eigenfunctions. With (19) we obtain

$$I^{\lambda}_{\lambda^{(1)}\,\lambda^{(2)} \ldots\, \lambda^{(n)}} = \left(\frac{1}{\sqrt{L}} \right)^{n-1} \delta_{\lambda^{(1)}+\lambda^{(2)}+\ldots+\lambda^{(n)},\lambda} \, , \tag{24}$$

$$J_{\lambda^{(1)}\,\lambda^{(2)} \ldots\, \lambda^{(n)}} = \left(\frac{1}{\sqrt{L}} \right)^{n-2} \delta_{\lambda^{(1)}+\lambda^{(2)}+\ldots+\lambda^{(n)},0} \, . \tag{25}$$

From these results one can immediately read off the special cases

$$I^{\lambda}_{\lambda'\,\lambda''} = \frac{1}{\sqrt{L}} \, \delta_{\lambda'+\lambda'',\lambda} \, , \tag{26}$$

$$I^{\lambda}_{\lambda'\,\lambda''\,\lambda'''} = \frac{1}{L} \, \delta_{\lambda'+\lambda''+\lambda''',\lambda} \, , \tag{27}$$

$$J_{\lambda'\,\lambda''} = \delta_{\lambda',-\lambda''} \, . \tag{28}$$

In (14) the integral (26) occurs only with unstable values of λ. As they can only differ by their sign, it follows $\lambda' + \lambda'' \neq \lambda$. Thus, we have $I^{\lambda}_{\lambda'\,\lambda''} = 0$, i.e. the quadratic term (14) in (11) vanishes:

$$A^{\lambda^u_T,\lambda^u_T{}'\lambda^u_T{}''}_{\lambda^u_R,\lambda^u_R{}'\lambda^u_R{}''} = 0 \, . \tag{29}$$

To arrive at a more concise representation, we split the cubic contribution in (11) in two terms according to

$$B^{\lambda^u_T,\lambda^u_T{}'\lambda^u_T{}''\lambda^u_T{}'''}_{\lambda^u_R,\lambda^u_R{}'\lambda^u_R{}''\lambda^u_R{}'''} U_{\lambda^u_T{}'\lambda^u_R{}'} \, U_{\lambda^u_T{}''\lambda^u_R{}''} \, U_{\lambda^u_T{}'''\lambda^u_R{}'''} = K_{1,\lambda^u_T\lambda^u_R} + K_{2,\lambda^u_T\lambda^u_R} \, . \tag{30}$$

The first term K_1 takes into account the contribution of the order parameters themselves, while the second term K_2 represents the influence of the center manifold on the order parameter dynamics. Applying the integrals (26)–(28) leads to selection rules for the appearance of cubic terms. It turns out that only those sums lead to non-vanishing contributions where the sum of three unstable modes $\lambda^{u'} + \lambda^{u''} + \lambda^{u'''}$ coincides with another unstable mode $\lambda^{u'}$. Thus, both for retina and tectum only the following combinations are allowed:

$$\left(\lambda^{u'}, \lambda^{u''}, \lambda^{u'''} \right) = (\lambda^u, \lambda^u, -\lambda^u) \; , \quad (\lambda^u, -\lambda^u, \lambda^u) \; , \quad (-\lambda^u, \lambda^u, \lambda^u) \; . \tag{31}$$

With this selection rule the first cubic term is given by

$$\begin{aligned} K_{1,\lambda^u_T\lambda^u_R} = & -\frac{f^T_{\lambda^u_T} f^R_{\lambda^u_R}}{2 L_T L_R} \Big[U_{\lambda^u_T\lambda^{u'}_R} U_{\lambda^{u''}_T\,\lambda^{u''}_R} U_{-\lambda^{u''}_T\,\lambda^{u'''}_R} \delta_{\lambda^{u'}_R+\lambda^{u''}_R+\lambda^{u'''}_R,\lambda^u_R} \\ & + U_{\lambda^{u'}_T\,\lambda^u_R} U_{\lambda^{u''}_T\,\lambda^{u''}_R} U_{\lambda^{u'''}_T-\lambda^{u''}_R} \delta_{\lambda^{u'}_T+\lambda^{u''}_T+\lambda^{u'''}_T,\lambda^u_T} \Big] \end{aligned} \tag{32}$$

and the second cubic term reads

$$\begin{aligned} K_{2,\lambda^u_T\lambda^u_R} = & \; H_{\lambda'_T\lambda'_R,\lambda^{u''}_T\lambda^{u''}_R\lambda^{u'''}_T\lambda^{u'''}_R} U_{\lambda^{u'}_T\,\lambda^{u'}_R} U_{\lambda^{u''}_T\,\lambda^{u''}_R} U_{\lambda^{u'''}_T\,\lambda^{u'''}_R} \left\{ \frac{f^T_{\lambda'_T} f^R_{\lambda'_R} + f^T_{\lambda^u_T} f^R_{\lambda^u_R}}{\sqrt{L_T L_R}} \delta_{\lambda^{u'}_T+\lambda'_T,\lambda^u_T} \delta_{\lambda^{u'}_R+\lambda'_R,\lambda^u_R} \right. \\ & \left. - \frac{1}{2\sqrt{L_T L_R}} \Big[(1 + f^R_{\lambda'_R}) \delta_{\lambda^{u'}_R+\lambda'_R,\lambda^u_R} \delta_{\lambda'_T 0} \delta_{\lambda^{u'}_T\,\lambda^u_T} + (1 + f^T_{\lambda'_T}) \delta_{\lambda^{u'}_T+\lambda'_T,\lambda^u_T} \delta_{\lambda'_R 0} \delta_{\lambda^{u'}_R\,\lambda^u_R} \Big] \right\} . \end{aligned} \tag{33}$$

The latter describes the influence of the center manifold, which follows from (17), (26), and (28) to be

$$
\begin{aligned}
H_{\lambda_T\lambda_R,\lambda_T^{u\prime\prime}\lambda_R^{u\prime\prime}\lambda_T^{u\prime\prime\prime}\lambda_R^{u\prime\prime\prime}} &= \frac{f^T_{\lambda_T^u} f^R_{\lambda_R^u}}{\sqrt{L_T L_R}\left(2\Lambda_{\lambda_T^u\lambda_R^u} - \Lambda_{\lambda_T\lambda_R}\right)} \Big[\delta_{\lambda_T^{u\prime\prime}+\lambda_T^{u\prime\prime\prime},\lambda_T}\delta_{\lambda_R^{u\prime\prime}+\lambda_R^{u\prime\prime\prime},\lambda_R} \\
&\quad -\frac{1}{2}\left(\delta_{\lambda_T^{u\prime\prime},-\lambda_T^{u\prime\prime\prime}}\delta_{\lambda_R^{u\prime\prime}+\lambda_R^{u\prime\prime\prime},\lambda_R}\delta_{\lambda_T 0} + \delta_{\lambda_R^{u\prime\prime},-\lambda_R^{u\prime\prime\prime}}\delta_{\lambda_T^{u\prime\prime}+\lambda_T^{u\prime\prime\prime},\lambda_T}\delta_{\lambda_R 0}\right)\Big] \,. \qquad (34)
\end{aligned}
$$

C. Complex Order Parameters

We can therefore conclude that the order parameter equations for strings have the form

$$\dot{U}_{\lambda_T^u\lambda_R^u} = h_{\lambda_T^u\lambda_R^u}(U,U^*) \qquad (35)$$

with the complex function

$$h_{\lambda_T^u\lambda_R^u}(U,U^*) = \Lambda_{\lambda_T^u\lambda_R^u}U_{\lambda_T^u\lambda_R^u} + A_{\lambda_T^u\lambda_R^u}U^2_{\lambda_T^u\lambda_R^u}U_{-\lambda_T^u-\lambda_R^u} + B_{\lambda_T^u\lambda_R^u}U_{\lambda_T^u\lambda_R^u}U_{-\lambda_T^u\lambda_R^u}U_{\lambda_T^u-\lambda_R^u} \,. \qquad (36)$$

Here we have introduced the coefficients

$$
\begin{aligned}
A_{\lambda_T^u\lambda_R^u} &= -\frac{\gamma}{L_T L_R}\left(2 - \frac{\gamma + \gamma^{2\lambda_T^u,2\lambda_R^u}}{2\Lambda_{\lambda_T^u\lambda_R^u} - \Lambda_{2\lambda_T^u,2\lambda_R^u}}\right) \,, \qquad (37)\\
B_{\lambda_T^u\lambda_R^u} &= -\frac{\gamma}{L_T L_R}\left[4 - \frac{\gamma + (\gamma^{2\lambda_T^u,0}-1)/2}{2\Lambda_{\lambda_T^u\lambda_R^u} - \Lambda_{2\lambda_T^u,0}} - \frac{\gamma + (\gamma^{0,2\lambda_R^u}-1)/2}{2\Lambda_{\lambda_T^u\lambda_R^u} - \Lambda_{0,2\lambda_R^u}}\right] \qquad (38)
\end{aligned}
$$

with the abbreviations $\gamma^{\lambda_T\lambda_R} := f^T_{\lambda_T} f^R_{\lambda_R}$ and $\gamma := \gamma^{\lambda_T^u,\lambda_R^u} = f^T_{\lambda_T^u} f^R_{\lambda_R^u}$. Now we turn to the question whether the order parameter equations (35) represent a potential dynamics. To this end we derived in Ref. [8] a condition for the order parameter equations which allows one to conclude whether or not such a potential exists. The potential criterion reads

$$\frac{\partial h_{\lambda_T^u\lambda_R^u}(U,U^*)}{\partial U_{\lambda_T^{u\prime}\lambda_R^{u\prime}}} = \frac{\partial h^*_{\lambda_T^{u\prime}\lambda_R^{u\prime}}(U,U^*)}{\partial U^*_{\lambda_T^u\lambda_R^u}} \,, \qquad (39)$$

which is, indeed, fulfilled for (36). Furthermore, we derived in Ref. [8] the following conditions for determining the underlying potential:

$$\dot{U}_{\lambda_T^u\lambda_R^u} = -\frac{1}{2}\frac{\partial V(U,U^*)}{\partial U^*_{\lambda_T^u\lambda_R^u}} \,. \qquad (40)$$

Integrating (40) yields the potential

$$
\begin{aligned}
V(U,U^*) &= -2\Lambda_{\lambda_T^u\lambda_R^u}\left(U_{\lambda_T^u\lambda_R^u}U_{-\lambda_T^u-\lambda_R^u} + U_{-\lambda_T^u\lambda_R^u}U_{\lambda_T^u-\lambda_R^u}\right) - A_{\lambda_T^u\lambda_R^u}\left(U^2_{\lambda_T^u\lambda_R^u}U^2_{-\lambda_T^u-\lambda_R^u} + U^2_{-\lambda_T^u\lambda_R^u}U^2_{\lambda_T^u-\lambda_R^u}\right) \\
&\quad -2B_{\lambda_T^u\lambda_R^u}U_{\lambda_T^u\lambda_R^u}U_{-\lambda_T^u-\lambda_R^u}U_{-\lambda_T^u\lambda_R^u}U_{\lambda_T^u-\lambda_R^u} \,. \qquad (41)
\end{aligned}
$$

D. Real Order Parameters

For technical purposes it has turned out to be useful to work with complex order parameters so far. However, in order to investigate their contribution to a one-to-one mapping between the strings, we have to transform them to real variables. We construct at first the real modes from the eigenfunctions (6), (19) of the linear operator $\hat{L}$ according to

$$
\begin{aligned}
c_{\lambda_T\lambda_R}(t,r) &= \frac{1}{2}\left[v_{\lambda_T\lambda_R}(t,r) + v_{-\lambda_T-\lambda_R}(t,r)\right] = \frac{1}{\sqrt{L_T L_R}}\cos\left(\frac{2\pi}{L_T}\lambda_T t + \frac{2\pi}{L_R}\lambda_R r\right) \,, \qquad (42)\\
s_{\lambda_T\lambda_R}(t,r) &= -\frac{i}{2}\left[v_{\lambda_T\lambda_R}(t,r) - v_{-\lambda_T-\lambda_R}(t,r)\right] = \frac{1}{\sqrt{L_T L_R}}\sin\left(\frac{2\pi}{L_T}\lambda_T t + \frac{2\pi}{L_R}\lambda_R r\right) \,. \qquad (43)
\end{aligned}
$$

These two modes span a real subspace. If we set

$$a = \rho \cos\psi\,, \quad b = \rho \sin\psi\,; \quad \rho \geq 0\,, \quad \psi \in (-\pi, \pi]\,, \tag{44}$$

the following relation results:

$$a\, c_{\lambda_T \lambda_R}(t,r) + b\, s_{\lambda_T \lambda_R}(t,r) = \rho \cos\left(\frac{2\pi}{L_T}\lambda_T t + \frac{2\pi}{L_R}\lambda_R r - \psi\right)\,. \tag{45}$$

Thus, the subspace consists of all phase-shifted functions of $\rho c_{\lambda_T \lambda_R}(t,r)$. Then the modes belonging to the unstable eigenvalue $(\lambda_T^u, \lambda_R^u)$ are given by the modes $c_{\lambda_T^u \lambda_R^u}(t,r)$ and $c_{\lambda_T^u - \lambda_R^u}(t,r)$ as well as all phase-shifted functions. Rewriting the unstable part (9)

$$U(t,r) = U_{\lambda_T^u \lambda_R^u} v_{\lambda_T^u \lambda_R^u}(t,r) + U_{-\lambda_T^u - \lambda_R^u} v_{-\lambda_T^u - \lambda_R^u}(t,r) + U_{\lambda_T^u - \lambda_R^u} v_{\lambda_T^u - \lambda_R^u}(t,r) + U_{-\lambda_T^u \lambda_R^u} v_{-\lambda_T^u \lambda_R^u}(t,r) \tag{46}$$

to real modes (42), (43), leads to

$$U(t,r) = u_1 c_{\lambda_T^u \lambda_R^u}(t,r) + u_2 s_{\lambda_T^u \lambda_R^u}(t,r) + u_3 c_{\lambda_T^u - \lambda_R^u}(t,r) + u_4 s_{\lambda_T^u - \lambda_R^u}(t,r)\,, \tag{47}$$

with real variables u_j:

$$\begin{aligned} u_1 &= U_{\lambda_T^u \lambda_R^u} + U_{-\lambda_T^u - \lambda_R^u}\,, \quad u_2 = i(U_{\lambda_T^u \lambda_R^u} - U_{-\lambda_T^u - \lambda_R^u})\,, \\ u_3 &= U_{\lambda_T^u - \lambda_R^u} + U_{-\lambda_T^u \lambda_R^u}\,, \quad u_4 = i(U_{\lambda_T^u - \lambda_R^u} - U_{-\lambda_T^u \lambda_R^u})\,. \end{aligned} \tag{48}$$

The inverse transformations are given by

$$\begin{aligned} U_{\lambda_T^u \lambda_R^u} &= (u_1 - iu_2)/2\,, \quad U_{-\lambda_T^u - \lambda_R^u} = (u_1 + iu_2)/2\,, \\ U_{\lambda_T^u - \lambda_R^u} &= (u_3 - iu_4)/2\,, \quad U_{-\lambda_T^u \lambda_R^u} = (u_3 + iu_4)/2\,. \end{aligned} \tag{49}$$

Inserting the transformations (49) into the complex potential (41), we obtain the following real potential

$$V(u_i) \;=\; -\frac{\Lambda_{\lambda_T^u \lambda_R^u}}{2}(u_1^2 + u_2^2 + u_3^2 + u_4^2) - \frac{A_{\lambda_T^u \lambda_R^u}}{16}\left[\left(u_1^2 + u_2^2\right)^2 + \left(u_3^2 + u_4^2\right)^2\right] - \frac{B_{\lambda_T^u \lambda_R^u}}{8}(u_1^2 + u_2^2)(u_3^2 + u_4^2)\,. \tag{50}$$

The corresponding equations of evolution for the real order parameters are determined from (50) with

$$\dot{u}_j = -\frac{\partial V(u_i)}{\partial u_j}\,. \tag{51}$$

They read explicitly

$$\begin{aligned} \dot{u}_1 &= \left[\Lambda_{\lambda_T^u \lambda_R^u} + \frac{A_{\lambda_T^u \lambda_R^u}}{4}(u_1^2 + u_2^2) + \frac{B_{\lambda_T^u \lambda_R^u}}{4}(u_3^2 + u_4^2)\right] u_1\,, \\ \dot{u}_2 &= \left[\Lambda_{\lambda_T^u \lambda_R^u} + \frac{A_{\lambda_T^u \lambda_R^u}}{4}(u_1^2 + u_2^2) + \frac{B_{\lambda_T^u \lambda_R^u}}{4}(u_3^2 + u_4^2)\right] u_2\,, \\ \dot{u}_3 &= \left[\Lambda_{\lambda_T^u \lambda_R^u} + \frac{A_{\lambda_T^u \lambda_R^u}}{4}(u_3^2 + u_4^2) + \frac{B_{\lambda_T^u \lambda_R^u}}{4}(u_1^2 + u_2^2)\right] u_3\,, \\ \dot{u}_4 &= \left[\Lambda_{\lambda_T^u \lambda_R^u} + \frac{A_{\lambda_T^u \lambda_R^u}}{4}(u_3^2 + u_4^2) + \frac{B_{\lambda_T^u \lambda_R^u}}{4}(u_1^2 + u_2^2)\right] u_4\,. \end{aligned} \tag{52}$$

E. Constant Phase Shift Angles

According to the remarks following Eq. (45), the unstable part (47) can be written as a superposition of two diagonal modes of different orientation

$$U(t,r) = \xi \cos\left[\frac{2\pi}{L_T}\lambda_T^u t + \frac{2\pi}{L_R}\lambda_R^u r - \psi\right] + \eta \cos\left[\frac{2\pi}{L_T}\lambda_T^u t - \frac{2\pi}{L_R}\lambda_R^u r - \varphi\right]\,. \tag{53}$$

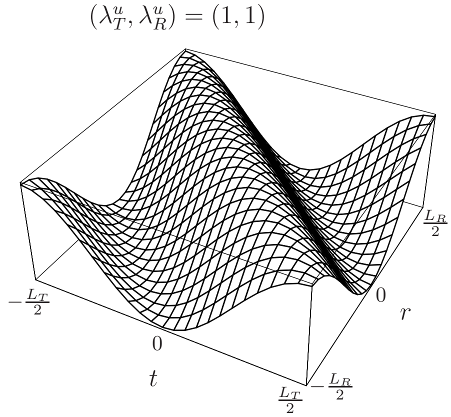

FIG. 2: Diagonal modes of different orientation according to (53) for the case $(\lambda_T^u, \lambda_R^u) = (1,1)$ and $(1,-1)$, respectively. Here the phase shift is set to $\psi = \varphi = 0$.

as is illustrated in Figure 2. With (44) and (45) we have

$$u_1 = \xi \cos\psi\,, \quad u_2 = \xi \sin\psi\,, \quad u_3 = \eta\cos\varphi\,, \quad u_4 = \eta \sin\varphi\,. \tag{54}$$

Then the amplitudes of the phase-shift diagonal modes read

$$\xi = \sqrt{u_1^2 + u_2^2}\,, \qquad \eta = \sqrt{u_3^2 + u_4^2} \tag{55}$$

and the phase angles are given by

$$\tan\psi = \frac{u_1}{u_2}\,, \qquad \tan\varphi = \frac{u_3}{u_4}\,. \tag{56}$$

From the order parameter equations (52) it follows

$$\frac{\dot u_1}{\dot u_2} = \frac{u_1}{u_2}\,, \qquad \frac{\dot u_3}{\dot u_4} = \frac{u_3}{u_4}\,. \tag{57}$$

Thus, performing a separation of variables and a subsequent integration leads to the relation

$$\frac{u_1}{u_2} = \text{const}\,, \qquad \frac{u_3}{u_4} = \text{const.} \tag{58}$$

Consequently, the four real equations (52) are reduced to two equations for the mode amplitudes ξ and η:

$$\begin{aligned} \dot\xi &= \left(\Lambda_{\lambda_T^u\lambda_R^u} + \frac{A_{\lambda_T^u\lambda_R^u}}{4}\xi^2 + \frac{B_{\lambda_T^u\lambda_R^u}}{4}\eta^2\right)\xi\,, \\ \dot\eta &= \left(\Lambda_{\lambda_T^u\lambda_R^u} + \frac{A_{\lambda_T^u\lambda_R^u}}{4}\eta^2 + \frac{B_{\lambda_T^u\lambda_R^u}}{4}\xi^2\right)\eta\,. \end{aligned} \tag{59}$$

The corresponding potential is

$$V(\xi,\eta) = -\frac{\Lambda_{\lambda_T^u\lambda_R^u}}{2}(\xi^2+\eta^2) - \frac{A_{\lambda_T^u\lambda_R^u}}{16}(\xi^4+\eta^4) - \frac{B_{\lambda_T^u\lambda_R^u}}{8}\xi^2\eta^2\,. \tag{60}$$

Thus, we have reduced the four complex order parameter equations (35), (36) to two real order parameter equations (59) with the potential (60).

F. Monotonous Cooperativity Functions

So far our considerations are valid for arbitrary unstable modes $(\lambda_T^u, \lambda_R^u)$. According to the eigenvalue spectrum (7) the unstable modes are determined by the expansion coefficients f_λ of the cooperativity functions. We therefore

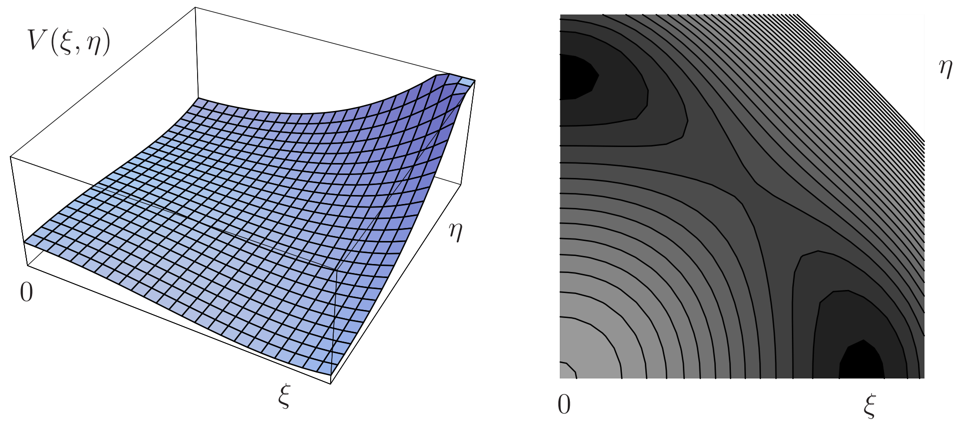

FIG. 3: The potential $V(\xi,\eta)$ according to Eq. (65) with $\Lambda > 0$. The originally stable state $\xi = \eta = 0$ becomes unstable. The system settles into one of the two minima, i.e. one of the two modes vanishes. The right plot shows the equipotential lines. Dark grey values correspond to small values of the potential V.

derive in this subsection some basic properties of these coefficients. In particular, we investigate the consequences of monotonically decreasing cooperativity functions for their expansion coefficients f_λ. As $c(x)$ is positive and normalized, we conclude $|f_\lambda| \leq 1$. Using the Euler formula and the symmetry $c(x) = c(-x)$, the expansion coefficients can be written in the form

$$f_\lambda = 2 \int_0^{L/2} c(x) \cos\left(\frac{2\pi}{L}\lambda x\right) dx\,, \tag{61}$$

which makes the symmetry $f_\lambda = f_{-\lambda}$ manifest. Integrating (61) by parts leads to

$$f_\lambda = -\frac{L}{\pi\lambda} \int_0^{L/2} c'(x) \sin\left(\frac{2\pi}{L}\lambda x\right) dx\,. \tag{62}$$

If we assume monotonically decreasing cooperativity functions, i.e. $dc/dx < 0$ for $x \in [0, L/2]$, we obtain $f_1 > 0$. Furthermore, we can show that f_1 is the largest expansion coefficient by considering the expression

$$f_1 - f_\lambda = -\frac{L}{\pi} \int_0^{L/2} c'(x) \left[\sin\left(\frac{2\pi}{L}x\right) - \frac{1}{\lambda}\sin\left(\frac{2\pi}{L}\lambda x\right)\right] dx\,. \tag{63}$$

Because of $c'(x) < 0$ and the obvious identity

$$\sin\left(\frac{2\pi}{L}x\right) \geq \frac{1}{\lambda}\sin\left(\frac{2\pi}{L}\lambda x\right) \tag{64}$$

for $x \in [0, L/2)$, it follows indeed $f_1 - f_\lambda > 0 \quad \forall\, \lambda \neq 0, \pm 1$. Together with $|f_\lambda| < 1$ the maximum eigenvalue of (7) results to be $\Lambda_{\max} = -\alpha + f_1^T f_1^R$. Hence in this case there are four unstable modes $(\lambda_T^u, \lambda_R^u) = (\pm 1, \pm 1)$, which corresponds to the result obtained in Ref. [3]. However, the most fundamental insight of our more general analysis is that the real order parameter equations (59) are also valid in the case where the cooperativity functions are not monotonic so that any mode $(\lambda_T^u, \lambda_R^u)$ can become unstable. It is plausible that there is a pathological development in animals which corresponds to this case.

G. Potential Properties

We now analyze the properties of the potential (60). For this purpose we restrict ourselves from now on to the unstable modes $(\lambda_T^u, \lambda_R^u) = (\pm 1, \pm 1)$, whose indices will be discarded for the sake of simplicity. Then the potential

(60) reads

$$V(\xi,\eta) = -\frac{\Lambda}{2}(\xi^2+\eta^2) - \frac{A}{16}(\xi^4+\eta^4) - \frac{B}{8}\xi^2\eta^2\,, \tag{65}$$

where the coefficients A, B follow from (37), (38) to be

$$A = -\frac{\gamma}{L_T L_R}\left(2 - \frac{\gamma+\gamma^{2,2}}{2\Lambda-\Lambda_{2,2}}\right), \tag{66}$$

$$B = -\frac{\gamma}{L_T L_R}\left[4 - \frac{\gamma+(\gamma^{2,0}-1)/2}{2\Lambda-\Lambda_{2,0}} - \frac{\gamma+(\gamma^{0,2}-1)/2}{2\Lambda-\Lambda_{0,2}}\right]. \tag{67}$$

From the condition $\nabla V = 0$ we determine the extrema of $V(\xi,\eta)$ and assign them to a minimum, a maximum, or a saddle point. In the unstable region with $\Lambda > 0$ the potential $V(\xi,\eta)$, which is depicted in Figure 3, has

- a relative maximum at $P_1(0,0)$,
- two relative minima at $P_2(0,\sqrt{-4\Lambda/A})$ and $P_3(\sqrt{-4\Lambda/A},0)$,
- a saddle point at $P_4(\sqrt{-4\Lambda/(A+B)},\sqrt{-4\Lambda/(A+B)})$.

In the stable region with $\Lambda < 0$ only the relative minimum $\xi = \eta = 0$ does exist. Initially, the system is in the stable uniform state $w_0(t,r) = 1$. This state becomes unstable if the control parameter α is decreased to the critical value $\alpha_c = f_1^T f_1^R$. The eigenvalue $\Lambda_{\max} = -\alpha + f_1^T f_1^R$ becomes positive, and the minimum passes into a maximum. The system settles into one of the two equivalent minima, i.e. a symmetry breaking takes place. Thereby the two modes compete with each other and, subsequently, one of the two modes vanishes. Which of them vanishes depends on the initial conditions of ξ and η. If the condition $\eta(0) > \xi(0)$ is fulfilled, the ξ-mode vanishes, and vice versa.

H. One-To-One Retinotopy

In the following we assume that, according to the potential dynamics discussed above, only one of the two modes remains. These two modes show a pronounced maximum for $t = -r$ and $t = r$, respectively, as is shown in Figure 2. To assess the influence of higher modes, we calculate the center manifold $S(U)$. We consider the case $\xi = 0$ and $\eta \neq 0$ and set $u_4 = 0$ without loss of generality. Then it follows from (55) that $\eta = u_3$, and we obtain for the unstable part (47)

$$U(t,r) = \eta\cos\left(\frac{2\pi}{L_T}t - \frac{2\pi}{L_R}r\right). \tag{68}$$

With the center manifold (34) the stable part (10), (16) reads explicitly

$$S(U) = \frac{2\gamma}{\sqrt{L_T L_R}\,(2\Lambda-\Lambda_{2,2})}\,\eta^2\cos\left(\frac{4\pi}{L_T}t - \frac{4\pi}{L_R}r\right). \tag{69}$$

Thus, those modes are excited which strengthen the retinotopic character of the projection. With the help of the complex modes it can be seen that this is also the case for higher modes, i.e. for $(\lambda_T^u,\lambda_R^u) = (1,1)$ exclusively the modes $(2,2)$, $(3,3)$ etc. are excited, which are depicted in Figure 4. Therefore, we follow Ref. [3] and use an ansatz which contains only diagonal modes and insert it into the Häussler equations (1). If we restrict ourselves to special cooperativity functions, the resulting recursion relations can be solved analytically by using the method of generating function. Note that our derivation of the solution of the recursion relations corresponds to the gravitating chain in Ref. [3].

1. *Recursion Relations*

Motivated by the above remarks we investigate the Häussler equations for strings with the ansatz

$$w(t,r) = \sqrt{L_T L_R}\sum_{\lambda=-\infty}^{\infty} w_\lambda v_{\lambda,-\lambda}(t,r)\,, \tag{70}$$

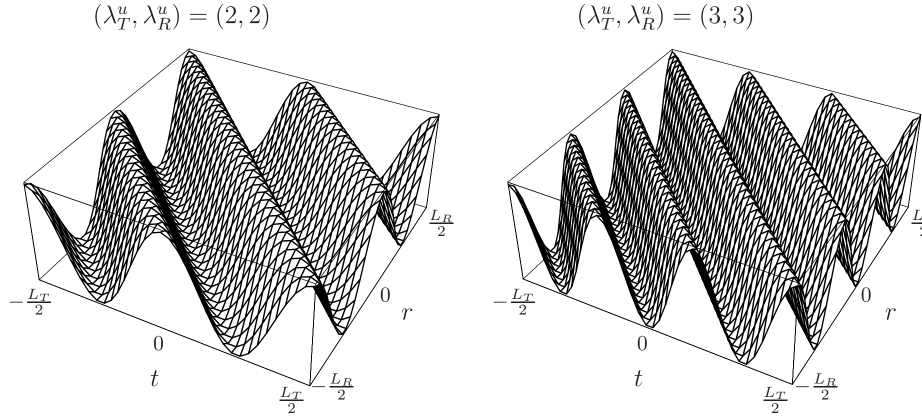

FIG. 4: Higher diagonal modes, which are excited by the unstable mode $(\lambda_T^u, \lambda_R^u) = (1,1)$ of Figure 2. They amplify the retinotopic character of the $(1,1)$-mode.

where $v_{\lambda,-\lambda}(t,r)$ is defined by (6) and (19). Thus, taking into account the decomposition (23) of the cooperativity functions, the Häussler equations (1) can be written as

$$\dot{w}(t,r) = -\alpha[w(t,r)-1] + w(t,r)\sqrt{L_T L_R}\sum_{\lambda=-\infty}^{\infty} w_\lambda f_\lambda^T f_\lambda^R v_{\lambda,-\lambda}(t,r) - p(w)\, w(t,r)\,, \tag{71}$$

where we have introduced the abbreviation

$$p(w) = \sum_{\lambda=-\infty}^{\infty} w_{-j} w_j f_j^T f_j^R\,. \tag{72}$$

Inserting the ansatz (70) into (71) and comparing the coefficients of the linearily independent functions $v_{\lambda,-\lambda}(t,r)$ yields

$$\dot{w}_0 \;=\; -\left[\alpha + p(w)\right](w_0 - 1)\,, \tag{73}$$

$$\dot{w}_\lambda \;=\; -\left[\alpha + p(w)\right] w_\lambda + \sum_{j=-\infty}^{\infty} w_{\lambda-j} w_j f_j^T f_j^R\,, \quad \lambda \neq 0\,. \tag{74}$$

As $w(t,r)$ is positive [1], we obtain that $p(w) > 0$ and $\alpha + p(w) > 0$. Therefore, the stationary state is determined from (73) to be

$$w_0 = 1\,. \tag{75}$$

2. *Special Cooperativity Functions*

We restrict our further considerations to the following form of the cooperativity functions (23):

$$\begin{aligned} c_T(t-t') &= \frac{1}{L_T}\left\{1 + 2f_1^T \cos\left[\frac{2\pi}{L_T}(t-t')\right]\right\}\,, \\ c_R(r-r') &= \frac{1}{L_R}\left\{1 + 2f_1^R \cos\left[\frac{2\pi}{L_R}(r-r')\right]\right\}\,. \end{aligned} \tag{76}$$

Thus, we assume $f_{\lambda_T}^T, f_{\lambda_R}^R = 0$ if $\lambda_T, \lambda_R \neq 0, \pm 1$. With the abbreviation $\gamma := f_1^T f_1^R$ the previous result (72) can be written as

$$p(w) = 1 + 2\gamma w_1 w_{-1}\,, \tag{77}$$

so that the equations (74) reduce to

$$\dot{w}_\lambda = -\left(\alpha + 2\gamma w_1 w_{-1}\right) w_\lambda + \gamma\left(w_1 w_{\lambda-1} + w_{-1} w_{\lambda+1}\right), \quad \lambda \neq 0\,. \tag{78}$$

For the stationary case (78) this leads to the recursion relation

$$(\alpha + 2\gamma w_1^2) w_\lambda = \gamma w_1 (w_{\lambda-1} + w_{\lambda+1})\,, \quad \lambda \neq 0\,. \tag{79}$$

3. Generating Function

To solve the recursion relations (79), we define the generating function

$$E(z) = \sum_{\lambda=-\infty}^{\infty} w_\lambda z^\lambda \,. \tag{80}$$

Multiplying (79) with $z^\lambda + z^{-\lambda}$ and performing the sum from $\lambda = 1$ up to infinity yields

$$(\alpha + 2\gamma w_1^2)[E(z) - w_0] = \gamma w_1 z \left[E(z) - \frac{w_1}{z} \right] + \gamma w_1 \left[\frac{E(z)}{z} - w_1 \right] \,. \tag{81}$$

This linear algebraic equation is solved by

$$E(z) = \frac{\alpha}{\alpha + 2\gamma w_1^2 - \gamma w_1 \left(z + z^{-1}\right)} \,. \tag{82}$$

To determine the coefficients w_λ we expand the generating function (82) into a Taylor series:

$$E(z) = -\frac{\alpha}{(\alpha + 2\gamma w_1^2)\, w \left(z_1 - z_1^{-1}\right)} \left[\sum_{\lambda=1}^{\infty} z_1^\lambda (z^\lambda + z^{-\lambda}) + 1 \right] , \quad |z_1| < |z| < |z_1|^{-1} \tag{83}$$

with the abbreviations

$$w = \frac{\gamma w_1}{\alpha + 2\gamma w_1^2} \,, \qquad z_1 = \frac{1}{2w}(1 + \sqrt{1 - 4w^2}\,) \,. \tag{84}$$

Comparing (83) with (80) by taking into account (75) leads at first to the condition

$$\frac{\alpha}{(\alpha + 2\gamma w_1^2)\, w \left(z_1 - z_1^{-1}\right)} = 1 \,, \tag{85}$$

which determines w_1 to be

$$w_1 = \sqrt{\frac{\gamma - \alpha}{\gamma}} \,. \tag{86}$$

Thus, together with (84) it follows $z_1 = w_1$, and the remaining coefficients turn out to be

$$w_\lambda = w_1^{|\lambda|} \,, \tag{87}$$

which is valid not only for $\lambda \neq 0$ but also for $\lambda = 0$ due to (75).

4. Limiting Cases

By inserting (87) into (70) we obtain the result

$$w_0(t, r) = \frac{1 - w_1^2}{1 - 2w_1 \cos\left(\frac{2\pi}{L_T} t - \frac{2\pi}{L_R} r\right) + w_1^2} \,. \tag{88}$$

For $w_1 = 0$ the stationary uniform state reduces to

$$w_0(t, r) = 1 \quad \forall t \in [0, L_T) \,,\, r \in [0, L_R) \,. \tag{89}$$

To investigate $w_0(t, r)$ for $w_1 = 1$, i.e. $w_\lambda = 1\ \forall\lambda$, we consider the expression

$$w_0(t, r) = \sum_{\lambda=-\infty}^{\infty} \exp\left[i2\pi\lambda \left(\frac{t}{L_T} - \frac{r}{L_R} \right) \right] \,. \tag{90}$$

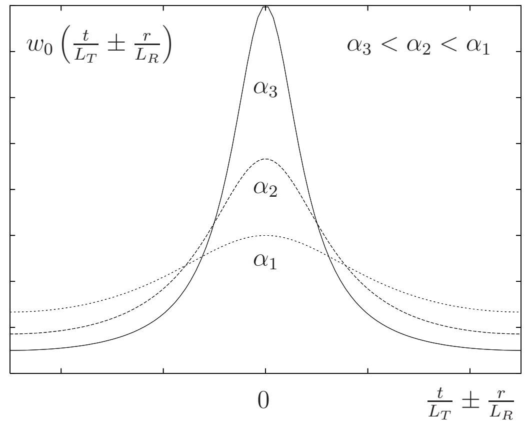

FIG. 5: Decreasing the control parameter α to smaller values, we read off from (86) and (88) that the connection weight converges to Dirac's delta function (91).

With the help of the Poisson formula [7] we find

$$w_0(t,r) = \delta\left(\frac{t}{L_T} - \frac{r}{L_R}\right). \tag{91}$$

Hence we have a situation which is illustrated in Figure 5: If the control parameter α is in the neighborhood of γ, the connection weight is essentially uniform with a small maximum for $t/L_T = \pm r/L_R$. Further decreasing of α leads to a sharpening of the projection. In the case $\alpha \to 0$ the projection becomes Dirac's delta function, i.e. a perfect one-to-one retinotopy is achieved. This means that the undifferentiated growth of new synaptic contacts comes to an end when the ordered projection between retina and tectum is fully developed.

I. Comparison with Linear Chains

Finally, we compare our results for strings with those of Ref. [3] where retina and tectum were treated as linear chains consisting of N cells, respectively. In that reference, the order parameter equations read

$$\dot{U}_{ij} = [\Lambda - \gamma(2-a)U_{ij}U_{-i-j} + (4 - b' - b'')U_{i-j}U_{-ij}]U_{ij} \tag{92}$$

with the abbreviations

$$a = -\frac{\gamma + \gamma^{2,2}}{\Lambda_{22}}, \tag{93}$$

$$b' = -\frac{\gamma + (\gamma^{2,0} - 1)/2}{\Lambda_{20}}, \tag{94}$$

$$b'' = -\frac{\gamma + (\gamma^{0,2} - 1)/2}{\Lambda_{02}}. \tag{95}$$

The comparison of the coefficients A, B according to (66), (67) with $\gamma(2-a)$, $\gamma(4-b'-b'')$ exhibits two differences: the factor $1/L_T L_R$ in A and B as well as the term 2Λ in the denominator. The absence of the corresponding factor $1/N^2$ in Ref. [3] stems from the circumstance that the eigenfunctions were not normalized there. Physically more interesting is the appearance of the term 2Λ in the denominator of A, B. The reason for this is that we have used the mathematically correct equation for the center manifold (17), whereas in Ref. [3] the adiabatic approximation $\dot{S} = 0$ was used. However, this ad-hoc method for implementing the adiabatic approximation, which is frequently used in the literature, is only justified for real eigenvalues. As the eigenvalues of the strings are real, we deduce for the vicinity of the instability point the relation

$$\Lambda = -\alpha + \gamma \approx 0. \tag{96}$$

Thus, the coefficients (66), (67) turn into those of Ref. [3] and the adiabatic approximation $\dot{S} = 0$ can be applied here.

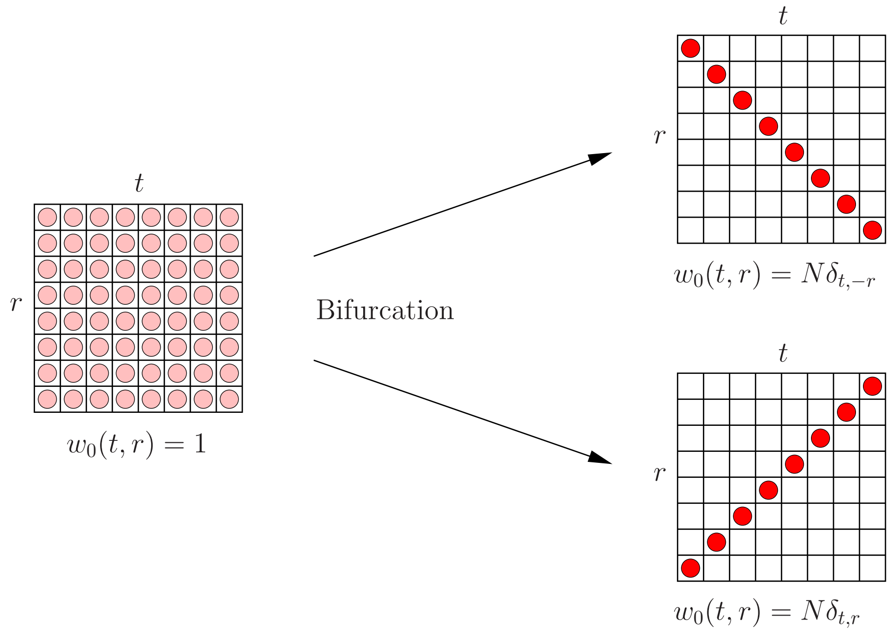

FIG. 6: Bifurcation in the vicinity of the instability point for the linear chain as analyzed in Ref. [3]. The quadratic arrangement of the two linear chains allows a concise representation of the connection weights. Dark gray means high connection weights between the corresponding cells t and r. At the uniform initial state all connection weights are equal. The bifurcation drives the system into one of the two possible states, which differ in their orientation. Decreasing the control parameter α to zero leads to a one-to-one retinotopy. Instead of a delta function in the continuous case, here the retinotopic order is described by Kronecker deltas.

Furthermore, our results for the continuous case are analogous to the results for discrete cell arrays. Also the transition to a perfect one-to-one retinotopy takes place in a corresponding way, as is illustrated in Figure 6. Thus, we conclude that our geometry-independent model for the emergence of retinotopic projections developed in Ref. [1] contains as a special case the results of Ref. [3]. In addition, we have extended the range of validity, i.e. the domain around the instability with $\Lambda = 0$, where the order parameter equations represent a quantitatively good approximation, as we have derived a more precise form of the center manifold (17).

IV. PLANES

In this section we extend our discussion to two dimensions where the cell sheets are assumed to be planes of side lengths L_1^T, L_2^T and L_1^R, L_2^R, respectively. To obtain a consistent solution we assume again periodic boundary conditions, i.e. the cell sheets are modelled as surfaces of tori. It turns out that we then have to calculate in total sixteen order parameter equations where the quadratic term vanishes, as in the case of strings, and where again selection rules reduce the number of cubic terms. This order parameter dynamics turns out to be complicated as the two dimensions do not decouple in a trivial way. Therefore, we have to restrict our analytical discussion of the order parameter dynamics to physiologically interesting special cases. If we set all modes to zero except for one, we find retinotopy only in one dimension. In a next step we consider the superposition of two retinotopic modes and investigate the necessary conditions for their coexistence. Such a situation occurs, for instance, when the cooperativity function of the tectum is monotonically decreasing, whereas the cooperativity function of the retina is not monotonic. Furthermore, we show that taking into account the center manifold contribution or higher modes leads to a sharpening of the retinotopic character of the projection between planar retina and tectum.

A. Eigenfunctions

In the following we consider both retina and tectum to be a planes with side lenghts L_1 and L_2. The points on the plane are represented by $x = (x_1, x_2)\,, x_1 \in [0, L_1)\,,\, x_2 \in [0, L_2)$. The magnitude of the plane is given by $M = L_1 L_2$.

The Laplace-Beltrami operator in Cartesian coordinates reads

$$\Delta = \frac{\partial^2}{\partial x_1^2} + \frac{\partial^2}{\partial x_2^2} \,. \tag{97}$$

The corresponding eigenvalue equation

$$\Delta\psi(x) = \chi\psi(x) \tag{98}$$

is solved for periodic boundary conditions, i.e. $\psi_j(x_j) = \psi_j(x_j + L_j)$ by the complete orthonormal system of eigenfunctions

$$\psi_\lambda(x) = \frac{1}{\sqrt{L_1 L_2}} \exp\left[2\pi i \left(\frac{\lambda_1 x_1}{L_1} - \frac{\lambda_2 x_2}{L_2}\right)\right] , \tag{99}$$

where $\lambda = (\lambda_1, \lambda_2)$. The cooperativity function $c(x - x')$ is expanded according to (3) in this basis:

$$c(x - x') = \frac{1}{L_1 L_2} \sum_{\lambda_1,\lambda_2} f_{(\lambda_1,\lambda_2)} \exp\left\{2\pi i \left[\frac{\lambda_1(x_1 - x_1')}{L_1} - \frac{\lambda_2(x_2 - x_2')}{L_2}\right]\right\} . \tag{100}$$

Note that again the expansion coefficients $f_{(\lambda_1,\lambda_2)}$ of the cooperativity functions are independent of the signs of the parameters λ_1, λ_2, as the cooperativity functions should be symmetric with respect to their arguments: $c(x - x') = c(x' - x)$. This requirement and the linear independence of the exponential functions leads to $f_{(\lambda_1,\lambda_2)} = f_{(\pm\lambda_1,\pm\lambda_2)}$. From now on we assume that the cooperativity functions decouple with respect to the two dimensions:

$$c(x - x') = c_1(x_1 - x_1')c_2(x_2 - x_2') \,. \tag{101}$$

As the individual cooperativity functions can be expanded according to

$$\begin{aligned} c_1(x_1 - x_1') &= \frac{1}{L_1} \sum_{\lambda_1} f_{\lambda_1} \exp\left[i\frac{2\pi}{L_1}\lambda_1(x_1 - x_1')\right] , \\ c_2(x_2 - x_2') &= \frac{1}{L_2} \sum_{\lambda_2} f_{\lambda_2} \exp\left[i\frac{2\pi}{L_2}\lambda_2(x_2 - x_2')\right] , \end{aligned} \tag{102}$$

the decoupling (101) amounts to a factorization of the expansion coefficients:

$$f_{(\lambda_1,\lambda_2)} = f_{\lambda_1} f_{\lambda_2} \,. \tag{103}$$

With this we allow for both anisotropic and isotropic cooperativity functions. This is an interesting feature as it is reasonable to assume that real cell sheets have a preferential direction.

B. Instability Point

We analyze which modes become unstable. According to (7) this depends on the expansion coefficients and the maximum eigenvalues are given by

$$\Lambda_{\lambda_T^u \lambda_R^u} = -\alpha + f^T_{\lambda_T^u} f^R_{\lambda_R^u} \,. \tag{104}$$

By doing so we require that all unstable modes become unstable *simultaneously*. This requirement is due to the fact that the order parameter equations should be approximately valid in the vicinity of the instability point. If the eigenvalues of the corresponding unstable modes would differ significantly, the situation that all modes are in the unstable region would have the consequence that the maximum eigenvalue would be larger than zero, i.e. far away from the instability point. Thus, the order parameter equations would be no adequate approximation. Consequently, we only consider the case that $\Lambda_{\lambda_T^u \lambda_R^u} = \Lambda_{\lambda_T^{u'} \lambda_R^{u'}}\ \forall \lambda_T^u, \lambda_R^u, \lambda_T^{u'}, \lambda_R^{u'}$, from which follows $f^T_{\lambda_T^u} = f^T_{\lambda_T^{u'}}$, $f^R_{\lambda_R^u} = f^R_{\lambda_R^{u'}}\ \forall \lambda_T^u, \lambda_R^u, \lambda_T^{u'}, \lambda_R^{u'}$. However, it is possible that $f^T_{\lambda_T^u} \neq f^R_{\lambda_R^u}$. From now on the unstable modes are assumed to be given by

$$\lambda^u = (1,0), (-1,0), (0,1), (0,-1) \,. \tag{105}$$

This occurs, for instance, for monotonically decreasing cooperativity functions where we obtain the relation $f_1^T > f_\lambda^T$ ($\lambda \neq 0, \pm 1$), by analogy with strings (see Section III F). Then the maximum expansion coefficient is given by $f_{\lambda^u} = f_{(\lambda_1^u,\lambda_2^u)} = f_{\lambda_1^u} f_{\lambda_2^u}$ for $\lambda_1^u = 0, \lambda_2^u = \pm 1$ and $\lambda_1^u = \pm 1, \lambda_2^u = 0$, respectively. Note, however, that the unstable modes (105) could also arise for non-monotonic cooperativity functions as we will see below.

C. Order Parameter Equations

We specialize the order parameter equations (11) to planes. At first we determine the integrals (12), (13) of products of eigenfunctions (99), which read

$$\begin{aligned} I^{\lambda}_{\lambda^{(1)}\lambda^{(2)}\ldots\lambda^{(n)}} &= \left(\frac{1}{L_1 L_2}\right)^{(n-1)/2} \delta_{\lambda^{(1)}+\lambda^{(2)}+\ldots+\lambda^{(n)},\lambda} \,, && (106)\\ J_{\lambda^{(1)}\lambda^{(2)}\ldots\lambda^{(n)}} &= \left(\frac{1}{L_1 L_2}\right)^{(n-2)/2} \delta_{\lambda^{(1)}+\lambda^{(2)}+\ldots+\lambda^{(n)},0} \,. && (107)\end{aligned}$$

For the order parameter equations (11) we need in (14), (15), (17) the special cases

$$\begin{aligned} I^{\lambda}_{\lambda'\,\lambda''} &= \frac{1}{\sqrt{L_1 L_2}}\,\delta_{\lambda'+\lambda'',\lambda} \,, && (108)\\ I^{\lambda}_{\lambda'\,\lambda''\,\lambda'''} &= \frac{1}{L_1 L_2}\,\delta_{\lambda'+\lambda''+\lambda''',\lambda} \,, && (109)\\ J_{\lambda'\,\lambda''} &= \delta_{\lambda',-\lambda''} \,. && (110)\end{aligned}$$

Note that the unstable modes (105) have the property $\lambda^{u'} + \lambda^{u''} \neq \lambda^u$. Thus, the quadratic coefficient (14) vanishes due to (108):

$$A^{\lambda^u_T,\lambda^u_T{}'\lambda^u_T{}''}_{\lambda^u_R,\lambda^u_R{}'\lambda^u_R{}''} = 0\,. \tag{111}$$

To yield a concise calculation of the order parameter equations, we introduce modes $\bar{\lambda}^u$ which are complementary to the unstable modes λ^u by permuting the two components:

$$\bar{\lambda}^u = \begin{cases} (0,\pm 1) & \text{if } \lambda^u = (\pm 1, 0)\,,\\ (\pm 1, 0) & \text{if } \lambda^u = (0,\pm 1)\,. \end{cases} \tag{112}$$

The integrals (108)–(110) involve selection rules for the appearance of cubic terms (15) which are analogous to those for strings. This condition turns out to be $\lambda^{u'} + \lambda^{u''} + \lambda^{u'''} = \lambda^u$ for (105), which leads to the following nine possibilities:

$$\begin{aligned} (\lambda^{u'},\lambda^{u''},\lambda^{u'''}) \;=\; & (\lambda^u,\lambda^u,-\lambda^u),(\lambda^u,-\lambda^u,\lambda^u),(-\lambda^u,\lambda^u,\lambda^u),(\lambda^u,\bar{\lambda}^u,-\bar{\lambda}^u),(\bar{\lambda}^u,\lambda^u,-\bar{\lambda}^u),\\ & (\bar{\lambda}^u,-\bar{\lambda}^u,\lambda^u),(\lambda^u,-\bar{\lambda}^u,\bar{\lambda}^u),(-\bar{\lambda}^u,\lambda^u,\bar{\lambda}^u),(-\bar{\lambda}^u,\bar{\lambda}^u,\lambda^u)\,. \end{aligned} \tag{113}$$

Combining the nine possible combinations for the tectum $(\lambda^{u'}_T, \lambda^{u''}_T, \lambda^{u'''}_T)$ with corresponding nine combinations for the retina $(\lambda^{u'}_R, \lambda^{u''}_R, \lambda^{u'''}_R)$ yields in total 81 combinations. However, some of these combinations are identical. To determine the number of *different* cubic terms $U_{\lambda^{u'}_T \lambda^{u'}_R} U_{\lambda^{u''}_T \lambda^{u''}_R} U_{\lambda^{u'''}_T \lambda^{u'''}_R}$, we consider the following cases separately:

1. No complementary mode $(\pm\bar{\lambda}^u_T, \pm\bar{\lambda}^u_R)$ appears.
2. Two complementary modes with respect to the T-indices appear, but none with respect to the R-indices.
3. The inverse case appears: $0 \times \pm\bar{\lambda}^u_T, 2 \times \pm\bar{\lambda}^u_R$.
4. Two complementary modes with respect of the T- and R-indices appear, respectively.

In this way it can be shown that in total 14 possible cubic terms have to be taken into account. The resulting order parameter equations read

$$\begin{aligned} \dot{U}_{\lambda^u_T\lambda^u_R} \;=\; & c_1 (U_{\lambda^u_T\lambda^u_R})^2 U_{-\lambda^u_T-\lambda^u_R} + c_2 U_{\lambda^u_T\lambda^u_R} U_{-\lambda^u_T\lambda^u_R} U_{\lambda^u_T-\lambda^u_R} + c_3 \left(U_{\lambda^u_T\lambda^u_R} U_{\bar{\lambda}^u_T\lambda^u_R} U_{-\bar{\lambda}^u_T-\lambda^u_R} + U_{\lambda^u_T\lambda^u_R} U_{\bar{\lambda}^u_T-\lambda^u_R} U_{-\bar{\lambda}^u_T\lambda^u_R} \right)\\ & + c_4 U_{\bar{\lambda}^u_T\lambda^u_R} U_{\lambda^u_T-\lambda^u_R} U_{-\bar{\lambda}^u_T\lambda^u_R} + c_5 \left(U_{\lambda^u_T\lambda^u_R} U_{\lambda^u_T\bar{\lambda}^u_R} U_{-\lambda^u_T-\bar{\lambda}^u_R} + U_{\lambda^u_T\lambda^u_R} U_{-\lambda^u_T\bar{\lambda}^u_R} U_{\lambda^u_T-\bar{\lambda}^u_R} \right)\\ & + c_6 U_{-\lambda^u_T\lambda^u_R} U_{\lambda^u_T\bar{\lambda}^u_R} U_{\lambda^u_T-\bar{\lambda}^u_R} + c_7 \left(U_{\lambda^u_T\lambda^u_R} U_{\bar{\lambda}^u_T\bar{\lambda}^u_R} U_{-\bar{\lambda}^u_T-\bar{\lambda}^u_R} + U_{\lambda^u_T\lambda^u_R} U_{\bar{\lambda}^u_T-\bar{\lambda}^u_R} U_{-\bar{\lambda}^u_T\bar{\lambda}^u_R} \right)\\ & + c_8 \Big(U_{\bar{\lambda}^u_T\lambda^u_R} U_{\lambda^u_T\bar{\lambda}^u_R} U_{-\bar{\lambda}^u_T-\bar{\lambda}^u_R} + U_{-\bar{\lambda}^u_T\lambda^u_R} U_{\lambda^u_T\bar{\lambda}^u_R} U_{\bar{\lambda}^u_T-\bar{\lambda}^u_R}\\ & + U_{\bar{\lambda}^u_T\lambda^u_R} U_{\lambda^u_T-\bar{\lambda}^u_R} U_{-\bar{\lambda}^u_T\bar{\lambda}^u_R} + U_{-\bar{\lambda}^u_T\lambda^u_R} U_{\lambda^u_T-\bar{\lambda}^u_R} U_{\bar{\lambda}^u_T\bar{\lambda}^u_R} \Big)\,. \end{aligned} \tag{114}$$

With the abbreviation $\tilde{\gamma} = \gamma / M_T M_R$ the coefficients c_1–c_8 are given by:

$$c_1 \;=\; -2\tilde{\gamma} + \frac{\tilde{\gamma}(\gamma^{2\lambda_T^u, 2\lambda_R^u} + \gamma)}{2\gamma - \gamma^{2\lambda_T^u, 2\lambda_R^u} - \alpha}\,, \tag{115}$$

$$c_2 \;=\; -4\tilde{\gamma} + \frac{\tilde{\gamma}(\gamma^{0,2\lambda_R^u} + 2\gamma - 1)}{2[2\gamma - (\gamma^{0,2\lambda_R^u} - 1)/2 - \alpha]} + \frac{\tilde{\gamma}(\gamma^{2\lambda_T^u,0} + 2\gamma - 1)}{2[2\gamma - (\gamma^{2\lambda_T^u,0} - 1)/2 - \alpha]} \tag{116}$$

$$c_3 \;=\; -3\tilde{\gamma} + \frac{\tilde{\gamma}(\gamma^{\lambda_T^u + \bar{\lambda}_T^u,0} + 2\gamma - 1)}{2[2\gamma - (\gamma^{\lambda_T^u + \bar{\lambda}_T^u,0} - 1)/2 - \alpha]} + \frac{2\tilde{\gamma}(\gamma + \gamma^{\lambda_T^u + \bar{\lambda}_T^u, 2\lambda_R^u})}{2\gamma - \gamma^{\lambda_T^u + \bar{\lambda}_T^u, 2\lambda_R^u} - \alpha}\,, \tag{117}$$

$$c_4 \;=\; -3\tilde{\gamma} + \frac{\tilde{\gamma}(\gamma^{0,2\lambda_R^u} + 2\gamma - 1)}{2[2\gamma - (\gamma^{0,2\lambda_R^u} - 1)/2 - \alpha]} + \frac{\tilde{\gamma}(\gamma^{\lambda_T^u + \bar{\lambda}_T^u,0} + 2\gamma - 1)}{2\gamma - (\gamma^{\lambda_T^u + \bar{\lambda}_T^u,0} - 1)/2 - \alpha} \tag{118}$$

$$c_5 \;=\; -3\tilde{\gamma} + \frac{\tilde{\gamma}(\gamma^{0,\lambda_R^u + \bar{\lambda}_R^u} + 2\gamma - 1)}{2[2\gamma - (\gamma^{0,\lambda_R^u + \bar{\lambda}_R^u} - 1)/2 - \alpha]} + \frac{2\tilde{\gamma}(\gamma + \gamma^{2\lambda_T^u, \lambda_R^u + \bar{\lambda}_R^u})}{2\gamma - \gamma^{2\lambda_T^u, \lambda_R^u + \bar{\lambda}_R^u} - \alpha}\,, \tag{119}$$

$$c_6 \;=\; -3\tilde{\gamma} + \frac{\tilde{\gamma}(\gamma^{2\lambda_T^u,0} + 2\gamma - 1)}{2[2\gamma - (\gamma^{2\lambda_T^u,0} - 1)/2 - \alpha]} + \frac{\tilde{\gamma}(\gamma^{0,\lambda_R^u + \bar{\lambda}_R^u} + 2\gamma - 1)}{2\gamma - (\gamma^{0,\lambda_R^u + \bar{\lambda}_R^u} - 1)/2 - \alpha} \tag{120}$$

$$c_7 \;=\; -2\tilde{\gamma} + \frac{4\tilde{\gamma}(\gamma + \gamma^{\lambda_T^u + \bar{\lambda}_T^u, \lambda_R^u + \bar{\lambda}_R^u})}{2\gamma - \gamma^{\lambda_T^u + \bar{\lambda}_T^u, \lambda_R^u + \bar{\lambda}_R^u} - \alpha}\,, \tag{121}$$

$$c_8 \;=\; -2\tilde{\gamma} + \frac{\tilde{\gamma}(\gamma^{\lambda_T^u + \bar{\lambda}_T^u,0} + 2\gamma - 1)}{2[2\gamma - (\gamma^{\lambda_T^u + \bar{\lambda}_T^u,0} - 1)/2 - \alpha]} + \frac{\tilde{\gamma}(\gamma^{0,\lambda_R^u + \bar{\lambda}_R^u} + 2\gamma - 1)}{2[2\gamma - (\gamma^{0,\lambda_R^u + \bar{\lambda}_R^u} - 1)/2 - \alpha]} + \frac{2\tilde{\gamma}(\gamma + \gamma^{\lambda_T^u + \bar{\lambda}_T^u, \lambda_R^u + \bar{\lambda}_R^u})}{2\gamma - \gamma^{\lambda_T^u + \bar{\lambda}_T^u, \lambda_R^u + \bar{\lambda}_R^u} - \alpha}\,. \tag{122}$$

Note that the first term proportional to $\tilde{\gamma}$ in the coefficients stems from the order parameters themselves, whereas the subsequent terms describe the influence of the center manifold.

D. Real Variables

To investigate how the complex order parameters contribute to the one-to-one-retinotopy between the planes, we have to transform them to real variables. To this end we introduce the transformation

$$u_{\lambda_T^u \lambda_R^u} = U_{\lambda_T^u \lambda_R^u} + U_{-\lambda_T^u - \lambda_R^u}\,, \qquad v_{\lambda_T^u \lambda_R^u} = i(U_{\lambda_T^u \lambda_R^u} - U_{-\lambda_T^u - \lambda_R^u}) \tag{123}$$

which is inverted according to

$$U_{\lambda_T^u \lambda_R^u} = (u_{\lambda_T^u \lambda_R^u} - i v_{\lambda_T^u \lambda_R^u})/2\,, \qquad U_{-\lambda_T^u - \lambda_R^u} = (u_{\lambda_T^u \lambda_R^u} + i v_{\lambda_T^u \lambda_R^u})/2\,. \tag{124}$$

With the help of the function

$$\begin{aligned} h_{\lambda_T^u \lambda_R^u, \lambda_T^{u\prime} \lambda_R^{u\prime}, \lambda_T^{u\prime\prime} \lambda_R^{u\prime\prime}}(u,v) \;:=\; & u_{\lambda_T^u \lambda_R^u} u_{\lambda_T^{u\prime} \lambda_R^{u\prime}} u_{\lambda_T^{u\prime\prime} \lambda_R^{u\prime\prime}} - u_{\lambda_T^u \lambda_R^u} v_{\lambda_T^{u\prime} \lambda_R^{u\prime}} v_{\lambda_T^{u\prime\prime} \lambda_R^{u\prime\prime}} \\ & + v_{\lambda_T^u \lambda_R^u} u_{\lambda_T^{u\prime} \lambda_R^{u\prime}} v_{\lambda_T^{u\prime\prime} \lambda_R^{u\prime\prime}} + v_{\lambda_T^u \lambda_R^u} v_{\lambda_T^{u\prime} \lambda_R^{u\prime}} u_{\lambda_T^{u\prime\prime} \lambda_R^{u\prime\prime}} \end{aligned} \tag{125}$$

the complex order parameter equations (114) are transformed to real ones as follows:

$$\begin{aligned} \dot{u}_{\lambda_T^u \lambda_R^u} \;=\; & u_{\lambda_T^u \lambda_R^u} \Big[c_1 \left(u^2_{\lambda_T^u \lambda_R^u} + v^2_{\lambda_T^u \lambda_R^u} \right) + c_2 \left(u^2_{\lambda_T^u - \lambda_R^u} + v^2_{\lambda_T^u - \lambda_R^u} \right) + c_3 \left(u^2_{\bar{\lambda}_T^u \lambda_R^u} + v^2_{\bar{\lambda}_T^u \lambda_R^u} + u^2_{\bar{\lambda}_T^u - \lambda_R^u} + v^2_{\bar{\lambda}_T^u - \lambda_R^u} \right) \\ & + c_5 \left(u^2_{\lambda_T^u \bar{\lambda}_R^u} + v^2_{\lambda_T^u \bar{\lambda}_R^u} + u^2_{\lambda_T^u - \bar{\lambda}_R^u} + v^2_{\lambda_T^u - \bar{\lambda}_R^u} \right) + c_7 \left(u^2_{\bar{\lambda}_T^u \bar{\lambda}_R^u} + v^2_{\bar{\lambda}_T^u \bar{\lambda}_R^u} + u^2_{\bar{\lambda}_T^u - \bar{\lambda}_R^u} + v^2_{\bar{\lambda}_T^u - \bar{\lambda}_R^u} \right) \Big] \\ & + c_6 h_{\lambda_T^u - \lambda_R^u, \lambda_T^u \bar{\lambda}_R^u, \lambda_T^u - \bar{\lambda}_R^u}(u,v) + c_8 \Big[h_{\bar{\lambda}_T^u \bar{\lambda}_R^u, \bar{\lambda}_T^u \lambda_R^u, \lambda_T^u \bar{\lambda}_R^u}(u,v) + h_{\bar{\lambda}_T^u - \lambda_R^u, \lambda_T^u \bar{\lambda}_R^u, \bar{\lambda}_T^u - \bar{\lambda}_R^u}(u,v) \\ & + h_{\bar{\lambda}_T^u - \bar{\lambda}_R^u, \lambda_T^u - \bar{\lambda}_R^u, \bar{\lambda}_T^u \lambda_R^u}(u,v) + h_{\bar{\lambda}_T^u - \lambda_R^u, \lambda_T^u - \bar{\lambda}_R^u, \bar{\lambda}_T^u \bar{\lambda}_R^u}(u,v) \Big]\,, \end{aligned} \tag{126}$$

$$\begin{aligned} \dot{v}_{\lambda_T^u \lambda_R^u} \;=\; & v_{\lambda_T^u \lambda_R^u} \Big[c_1 \left(u^2_{\lambda_T^u \lambda_R^u} + v^2_{\lambda_T^u \lambda_R^u} \right) + c_2 \left(u^2_{\lambda_T^u - \lambda_R^u} + v^2_{\lambda_T^u - \lambda_R^u} \right) + c_3 \left(u^2_{\bar{\lambda}_T^u \lambda_R^u} + v^2_{\bar{\lambda}_T^u \lambda_R^u} + u^2_{\bar{\lambda}_T^u - \lambda_R^u} + v^2_{\bar{\lambda}_T^u - \lambda_R^u} \right) \\ & + c_5 \left(u^2_{\lambda_T^u \bar{\lambda}_R^u} + v^2_{\lambda_T^u \bar{\lambda}_R^u} + u^2_{\lambda_T^u - \bar{\lambda}_R^u} + v^2_{\lambda_T^u - \bar{\lambda}_R^u} \right) + c_7 \left(u^2_{\bar{\lambda}_T^u \bar{\lambda}_R^u} + v^2_{\bar{\lambda}_T^u \bar{\lambda}_R^u} + u^2_{\bar{\lambda}_T^u - \bar{\lambda}_R^u} + v^2_{\bar{\lambda}_T^u - \bar{\lambda}_R^u} \right) \Big] \\ & + c_6 h_{\lambda_T^u - \lambda_R^u, \lambda_T^u \bar{\lambda}_R^u, \lambda_T^u - \bar{\lambda}_R^u}(v,u) + c_8 \Big[h_{\bar{\lambda}_T^u \bar{\lambda}_R^u, \bar{\lambda}_T^u \lambda_R^u, \lambda_T^u \bar{\lambda}_R^u}(v,u) + h_{\bar{\lambda}_T^u - \lambda_R^u, \lambda_T^u \bar{\lambda}_R^u, \bar{\lambda}_T^u - \bar{\lambda}_R^u}(u,v) \\ & + h_{\bar{\lambda}_T^u - \bar{\lambda}_R^u, \lambda_T^u - \bar{\lambda}_R^u, \bar{\lambda}_T^u \lambda_R^u}(v,u) + h_{\bar{\lambda}_T^u - \lambda_R^u, \lambda_T^u - \bar{\lambda}_R^u, \bar{\lambda}_T^u \bar{\lambda}_R^u}(v,u) \Big]\,. \end{aligned} \tag{127}$$

It can be shown that the order parameter dynamics (126), (127) is governed by a potential [8]. However, as the corresponding expression for the potential is very lengthy, we will not discuss it here explicitly. Instead, we investigate different analytical cases which depend on the number of non-vanishing modes. In particular, we are interested in the emergence of retinotopical ordered projections between the planes.

E. Retinotopic Projections: One Non-Vanishing Mode

We start with the assumption that only the amplitudes u_j, v_j of one mode are different from zero. We consider the case $j = 2$, but the other cases yield analogous results. The unstable part (9) reads

$$U(t,r) = U_{10,-10} \exp\left[i2\pi \left(\frac{t_1}{L_1^T} - \frac{r_1}{L_1^R} \right) \right] + U_{-10,10} \exp\left[-i2\pi \left(\frac{t_1}{L_1^T} - \frac{r_1}{L_1^R} \right) \right] . \tag{128}$$

which is equivalent to

$$U(t,r) = u_2 \cos\left[2\pi \left(\frac{t_1}{L_1^T} - \frac{r_1}{L_1^R} \right) \right] + v_2 \sin\left[2\pi \left(\frac{t_1}{L_1^T} - \frac{r_1}{L_1^R} \right) \right] , \tag{129}$$

The complex order parameter equations (114) reduce to

$$\begin{aligned} \dot{U}_{10,-10} &= \Lambda U_{10,-10} + c_1 U_{10,-10}^2 U_{-10,10} \,, \\ \dot{U}_{-10,10} &= \Lambda U_{-10,10} + c_1 U_{-10,10}^2 U_{10,-10} \,, \end{aligned} \tag{130}$$

and the corresponding real equations (126), (127) to

$$\begin{aligned} \dot{u}_2 &= \Lambda u_2 + \frac{c_1}{4} u_2 (u_2^2 + v_2^2) \,, \\ \dot{v}_2 &= \Lambda v_2 + \frac{c_1}{4} v_2 (u_2^2 + v_2^2) \,. \end{aligned} \tag{131}$$

Because of

$$\frac{\dot{u}_2}{\dot{v}_2} = \frac{u_2}{v_2} \tag{132}$$

we obtain constant phase-shift angles. With $\xi = \sqrt{u_2^2 + v_2^2}$ it follows

$$\dot{\xi} = \Lambda \xi + \frac{c_1}{4} \xi^3 \,. \tag{133}$$

For the stationary case this leads to

$$\xi = 0 \vee \xi = \sqrt{-\frac{4\Lambda}{c_1}} \,. \tag{134}$$

We are only interested in the case $\xi \neq 0$. This case corresponds to a retinotopy between r_1 and t_1, respectively. Thus, we have a retinotopic order only in one dimension and not in the whole plane.

F. Retinotopic Projections: Two Non-Vanishing Modes

Now we examine the question, if two modes are able to generate a retinotopic state in the plane. As a typical example we consider the case that u_2, v_2 as well as u_8, v_8 remain. Thus, the unstable part (9) has the complex decomposition

$$\begin{aligned} U(t,r) \;=\; & U_{10,-10} \exp\left[i2\pi \left(\frac{t_1}{L_1^T} - \frac{r_1}{L_1^R} \right) \right] + U_{-10,10} \exp\left[-i2\pi \left(\frac{t_1}{L_1^T} - \frac{r_1}{L_1^R} \right) \right] \\ & + U_{01,0-1} \exp\left[i2\pi \left(\frac{t_2}{L_2^T} - \frac{r_2}{L_2^R} \right) \right] + U_{0-1,01} \exp\left[-i2\pi \left(\frac{t_2}{L_2^T} - \frac{r_2}{L_2^R} \right) \right] , \end{aligned} \tag{135}$$

which due to (124) corresponds to the real decomposition

$$\begin{aligned} U(t,r) &= u_2 \cos\left[2\pi\left(\frac{t_1}{L_1^T} - \frac{r_1}{L_1^R}\right)\right] + v_2 \sin\left[2\pi\left(\frac{t_1}{L_1^T} - \frac{r_1}{L_1^R}\right)\right] \\ &\quad + u_8 \cos\left[2\pi\left(\frac{t_2}{L_2^T} - \frac{r_2}{L_2^R}\right)\right] + v_8 \sin\left[2\pi\left(\frac{t_2}{L_2^T} - \frac{r_2}{L_2^R}\right)\right] . \end{aligned} \tag{136}$$

For the complex order parameter equations (114) we obtain

$$\begin{aligned} \dot U_{10,-10} &= \Lambda U_{10,-10} + c_1 U_{10,-10}^2 U_{-10,10} + c_7 [U_{10,-10} U_{01,0-1} U_{0-1,01} + U_{10,-10} U_{01,01} U_{0-1,0-1}] , \\ \dot U_{-10,10} &= \Lambda U_{-10,10} + c_1 U_{-10,10}^2 U_{10,-10} + c_7 [U_{-10,10} U_{0-1,01} U_{01,0-1} + U_{-10,10} U_{0-1,0-1} U_{01,01}] , \\ \dot U_{01,0-1} &= \Lambda U_{01,0-1} + c_1 U_{01,0-1}^2 U_{0-1,01} + c_7 [U_{01,0-1} U_{10,-10} U_{-10,10} + U_{01,0-1} U_{10,10} U_{-10,-10}] , \\ \dot U_{0-1,01} &= \Lambda U_{0-1,01} + c_1 U_{0-1,01}^2 U_{01,0-1} + c_7 [U_{0-1,01} U_{-10,10} U_{10,-10} + U_{0-1,01} U_{-10,-10} U_{10,10}] , \end{aligned} \tag{137}$$

and therefore the real order parameter equations (126), (127) read

$$\begin{aligned} \dot u_2 &= \left[\Lambda + \frac{c_1}{4}(u_2^2 + v_2^2) + \frac{c_7}{4}(u_8^2 + v_8^2)\right] u_2 , \\ \dot v_2 &= \left[\Lambda + \frac{c_1}{4}(u_2^2 + v_2^2) + \frac{c_7}{4}(u_8^2 + v_8^2)\right] v_2 , \\ \dot u_8 &= \left[\Lambda + \frac{c_1}{4}(u_8^2 + v_8^2) + \frac{c_7}{4}(u_2^2 + v_2^2)\right] u_8 , \\ \dot v_8 &= \left[\Lambda + \frac{c_1}{4}(u_8^2 + v_8^2) + \frac{c_7}{4}(u_2^2 + v_2^2)\right] v_8 . \end{aligned} \tag{138}$$

Again we obtain constant phase-shift angles:

$$\frac{\dot u_2}{\dot v_2} = \frac{u_2}{v_2} , \quad \frac{\dot u_8}{\dot v_8} = \frac{u_8}{v_8} . \tag{139}$$

With the amplitudes

$$\xi = \sqrt{u_2^2 + v_2^2} , \quad \eta = \sqrt{u_8^2 + v_8^2} , \tag{140}$$

the following coupled equations result

$$\dot\xi = \left(\Lambda + \frac{c_1}{4}\xi^2 + \frac{c_7}{4}\eta^2\right)\xi , \qquad \dot\eta = \left(\Lambda + \frac{c_1}{4}\eta^2 + \frac{c_7}{4}\xi^2\right)\eta . \tag{141}$$

We investigate under which conditions the two retinotopic modes coexist. If $\xi, \eta \neq 0$, we obtain from $\dot\xi = \dot\eta = 0$ the relation

$$(\xi^2 - \eta^2)(c_1 - c_7) = 0 . \tag{142}$$

As we should minimize the restrictions for the coefficients c_1, c_7, we have in general $c_1 \neq c_7$, so we conclude $\xi = \eta$. Inserting this result in (141) for the stationary case leads to

$$\xi = \eta = \sqrt{-\frac{4\Lambda}{c_1 + c_7}} . \tag{143}$$

As the amplitudes ξ, η have to be real and $\Lambda > 0$, the coefficients c_1, c_7 have to fulfill the condition

$$c_1 + c_7 < 0 . \tag{144}$$

Furthermore, we require that the coexistence of both modes is stable. To this end we consider the potential

$$V(\xi, \eta) = -\frac{\Lambda}{2}(\xi^2 + \eta^2) - \frac{c_1}{16}(\xi^4 + \eta^4) - \frac{c_7}{8}\xi^2\eta^2 , \tag{145}$$

which reproduces according to

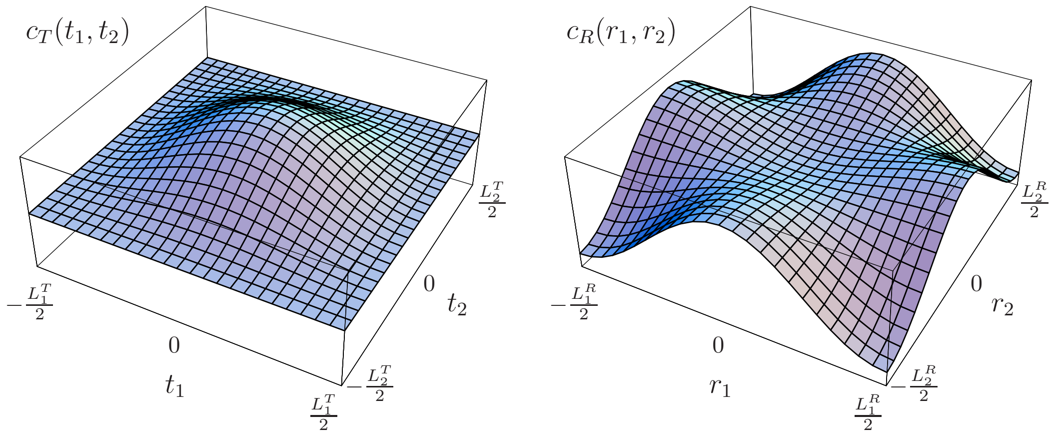

FIG. 7: Cooperativity functions for retina and tectum according to the special cases (153). The restriction to monotonically decreasing cooperativity functions has to be abandoned.

$$\dot{\xi} = -\frac{\partial V(\xi,\eta)}{\partial \xi}\,, \quad \dot{\eta} = -\frac{\partial V(\xi,\eta)}{\partial \eta} \tag{146}$$

the amplitude equations (141). A stable state corresponds to a minimum of the potential (145), which leads to the condition

$$c_1 - c_7 < 0\,. \tag{147}$$

According to the relations (115) and (121) the coefficients c_1 and c_7 read

$$c_1 = -2\gamma + \gamma\frac{\gamma+\gamma^{20,20}}{\gamma-\gamma^{20,20}}\,, \quad c_7 = -2\gamma + 4\gamma\frac{\gamma+\gamma^{11,11}}{\gamma-\gamma^{11,11}}\,. \tag{148}$$

Inserting these results into (144), (147) leads to the inequalities

$$\gamma(\gamma+\gamma^{20,20}) \;<\; \gamma^{11,11}(9\gamma^{20,20}-7\gamma)\,, \tag{149}$$

$$\gamma(3\gamma-5\gamma^{20,20}) \;>\; \gamma^{11,11}(3\gamma^{20,20}-5\gamma)\,. \tag{150}$$

One of the both coefficients $\gamma^{20,20}$ and $\gamma^{11,11}$ could vanish,

$$\gamma^{20,20}=0 \;\longrightarrow\; \gamma < -7\gamma^{11,11}\,, \quad \gamma > -5\gamma^{11,11}/3\,, \tag{151}$$

$$\gamma^{11,11}=0 \;\longrightarrow\; \gamma < -\gamma^{20,20}\,, \quad \gamma > 5\gamma^{20,20}/3\,, \tag{152}$$

but the simultaneous vanishing $\gamma^{20,20}=\gamma^{11,11}=0$ leads to the contradiction $\gamma^2<0$ and $\gamma^2>0$. As an example we consider the first case and assume special form of the cooperativity functions

$$\begin{aligned} c_T(t_1,t_2) &= 1+0.2\cos\left(\frac{2\pi t_1}{L_1^T}\right)+0.2\cos\left(\frac{2\pi t_2}{L_2^T}\right)+0.1\cos\left[2\pi\left(\frac{t_1}{L_1^T}+\frac{t_2}{L_2^T}\right)\right]+0.1\cos\left[2\pi\left(\frac{t_1}{L_1^T}-\frac{t_2}{L_2^T}\right)\right]\,, \\ c_R(r_1,r_2) &= 1+0.2\cos\left(\frac{2\pi r_1}{L_1^R}\right)+0.2\cos\left(\frac{2\pi r_2}{L_2^R}\right)-0.1\cos\left[2\pi\left(\frac{r_1}{L_1^R}+\frac{r_2}{L_2^R}\right)\right]-0.1\cos\left[2\pi\left(\frac{r_1}{L_1^R}-\frac{r_2}{L_2^R}\right)\right]\,. \end{aligned} \tag{153}$$

Thus, we have $f^T_{\pm10}=f^T_{0\pm1}=f^R_{\pm10}=f^R_{0\pm1}=0.1$, whereas the other expansion coefficients are different from each other: $f^T_{\pm1,\pm1}=0.05$, $f^R_{\pm1,\pm1}=-0.1$. Then it follows $\gamma=0.01$ and $\gamma^{11,11}=-0.005$, so that the requirements (151) are satisfied. However, this implies that, although the cooperativity function of the tectum is monotonically decreasing, the cooperativity function of the retina is not monotonic, as is illustrated in Figure 7. The corresponding potential (145) is shown in Figure 8.

G. Center Manifold

In the next step we analyze the influence of the center manifold $S(U)$ for the special case (151). With (8) the connection weight can be represented as

$$w(t,r) = 1 + U(t,r) + S(U(t,r))\,. \tag{154}$$

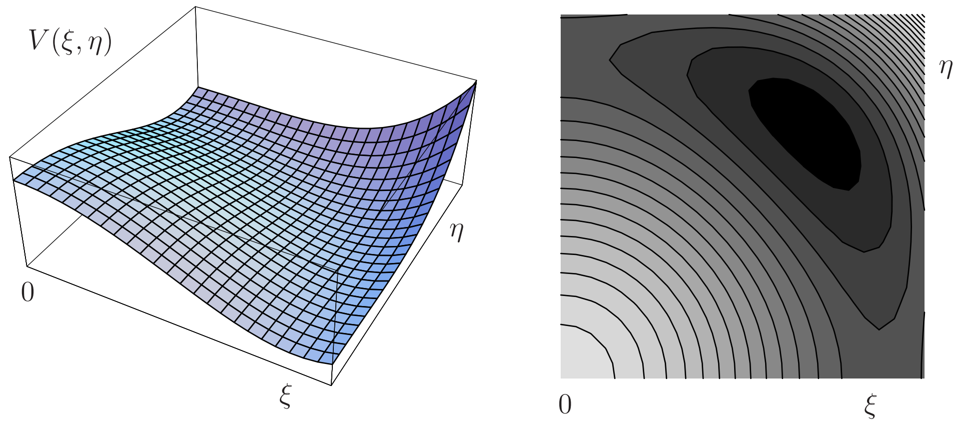

FIG. 8: The potential (145) for two coexistent retinotopic modes. According to (143) there is a maximum at $\xi = \eta = 0$ and a minimum at $\xi = \eta$. The right plot shows the equipotential lines, which pronounces the extrema of V.

Using the relations (16) and (17) the stable part is approximated in the second order:

$$
\begin{aligned}
S(U) \;=\; & \frac{1}{\sqrt{M_T M_R}} \Big[U^2_{10,-10} v_{20,-20}(t,r) + U^2_{-10,10} v_{-20,20}(t,r) + U^2_{01,0-1} v_{02,0-2}(t,r) + U^2_{0-1,01} v_{0-2,02}(t,r) \Big] \\
& + \frac{2\gamma}{\sqrt{M_T M_R}\,(\gamma - \gamma^{11,11})} \Big[U_{10,-10} U_{01,0-1} v_{11,-1-1}(t,r) + U_{-10,10} U_{0-1,01} v_{-1-1,11}(t,r) \\
& + U_{10,-10} U_{0-1,01} v_{1-1,-11}(t,r) + U_{-10,10} U_{01,0-1} v_{-11,1-1}(t,r) \Big] \,. \qquad (155)
\end{aligned}
$$

We rewrite this result to real variables and eigenfunctions, where we set $L_1^{T,R} = L_2^{T,R} = 2$. Then (155) results to

$$
\begin{aligned}
S(U) \;=\; & \frac{1}{32}(u_2^2 - v_2^2)\cos[2\pi(t_1 - r_1)] + \frac{1}{32}(u_8^2 - v_8^2)\cos[2\pi(t_2 - r_2)] + \frac{1}{16}\Big\{ u_2 v_2 \sin[2\pi(t_1 - r_1)] \\
& + u_8 v_8 \sin[2\pi(t_2 - r_2)] \Big\} + \frac{\gamma}{16(\gamma - \gamma^{11,11})} \Big(u_2 u_8 \big\{ \cos[\pi(t_1 - r_1 - t_2 + r_2)] + \cos[\pi(t_1 - r_1 + t_2 - r_2)] \big\} \\
& + v_2 v_8 \big\{ \cos[\pi(t_1 - r_1 - t_2 + r_2)] - \cos[\pi(t_1 - r_1 + t_2 - r_2)] \big\} + u_2 v_8 \big\{ \sin[\pi(t_1 - r_1 + t_2 - r_2)] \\
& - \sin[\pi(t_1 - r_1 - t_2 + r_2)] \big\} + u_8 v_2 \big\{ \sin[\pi(t_1 - r_1 - t_2 + r_2)] + \sin[\pi(t_1 - r_1 + t_2 - r_2)] \big\} \Big) \,. \qquad (156)
\end{aligned}
$$

In Figure 9 we compare $U(t,r)$ with $U(t,r) + S(U(t,r))$. It is evident that the retinotopic projection gets sharper due to the contribution of the center manifold, i.e. the projection is maximal around the point $t = r$. This corresponds to the situation found in the case of linear strings; the contribution of the higher modes have the tendency to support the emergence of retinotopic order.

V. SUMMARY

In this paper we have explicitly applied our generic model for the emergence of retinotopic projections between manifolds of different geometry to one- and two-dimensional Euclidean manifolds. By treating retina and tectum as strings we generalized the original approach of Häussler and von der Malsburg where both were modelled as one-dimensional discrete cell arrays. This change from discrete to continuous variables is physiologically reasonable because of the high cell density in vertebrate animals. By using a continuous instead of a discrete model we emphasized that we are not interested in the dynamics of the single cell but in the evolving global spatio-temporal patterns of the system. Furthermore, continuous variables are helpful to describe retinotopic projections between manifolds of different magnitudes as we have seen by the example of two strings of different lengths. In case of discrete cell arrays with different cell numbers it is not clear what a perfect retinotopy means, whereas in the continuous case a perfect one-to-one projection can be described without offending the bijectivity of the projections. Finally, as the one-dimensional string model could only serve as a simplistic approximation to the real biological situation, we have also investigated under which conditions retinotopic projections between planar networks of neurons arise. Obviously, this increase of the spatial dimension rendered the synergetic analysis so complicated that we were only able to treat

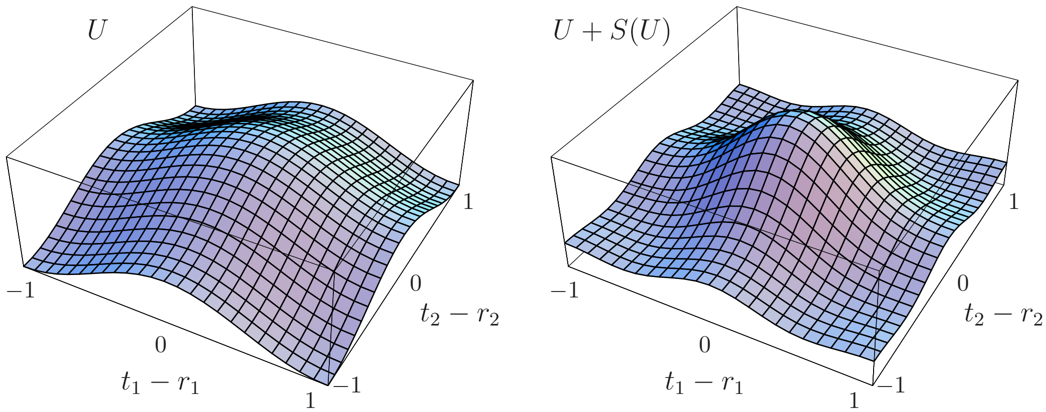

FIG. 9: The contribution of the center manifold (156) leads to a more distinct concentration of the connection weight $w(t, r) \approx 1 + U(t, r) + S(U(t, r))$ around $t = r$, as compared with the approximation $w(t, r) \approx 1 + U(t, r)$.

physiologically interesting special cases. While for strings retinotopy was only possible for monotonically decreasing cooperativity functions, we found that this is no longer true for planes.

---

[1] M. Güßmann, A. Pelster, and G. Wunner, *Self-Organized Formation of Retinotopic Projections Between Manifolds of Different Geometries – Part 2: The General Model;* preprint

[2] G.J. Goodhill and L.J. Richards, Trends Neurosci. **22**, 529 (1999)

[3] A.F. Häussler and C. von der Malsburg, J. Theoret. Neurobiol. **2**, 47 (1983)

[4] H. Haken, *Synergetics, An Introduction*, Third Edition, Springer, Berlin (1983)

[5] H. Haken, *Advanced Synergetics*, Springer, Berlin (1983)

[6] M. Güßmann, A. Pelster, and G. Wunner, *Self-Organized Development of Retinotopic Projections*; in U.J. Illg, H.H. Bülthoff and H.A. Mallot (Editors), *Proceedings of the 5. Workshop Dynamic Perception, Tübingen, Germany, November 18-19, 2004*; Akademische Verlagsgesellschaft Berlin, p. 239 (2004)

[7] H. Kleinert, *Path Integrals in Quantum Mechanics, Statistics, Polymer Physics and Financial Markets;* 3rd. ed. World Scientific, Singapore (2004)

[8] M. Güßmann, *Self-Organization between Manifolds of Euclidean and non-Euclidean Geometry by Cooperation and Competition*, Universität Stuttgart, Ph. D. Thesis (2006)